Effects of Vertical Wind Shear on the Intensity and Structure of Numerically Simulated Hurricanes

WILLIAM M. FRANK AND ELIZABETH A. RITCHIE*

Department of Meteorology, The Pennsylvania State University, University Park, Pennsylvania

(Manuscript received 5 April 2000, in final form 26 February 2001)

ABSTRACT

A series of numerical simulations of tropical cyclones in idealized large-scale environments is performed to examine the effects of vertical wind shear on the structure and intensity of hurricanes. The simulations are performed using the nonhydrostatic Pennsylvania State University–National Center for Atmospheric Research fifth-generation Mesoscale Model using a 5-km fine mesh and fully explicit representation of moist processes.

When large-scale vertical shears are applied to mature tropical cyclones, the storms quickly develop wavenumber one asymmetries with upward motion and rainfall concentrated on the left side of the shear vector looking downshear, in agreement with earlier studies. The asymmetries develop due to the storm's response to imbalances caused by the shear. The storms in shear weaken with time and eventually reach an approximate steady-state intensity that is well below their theoretical maximum potential intensity. As expected, the magnitude of the weakening increases with increasing shear. All of the storms experience time lags between the imposition of the large-scale shear and the resulting rise in the minimum central pressure. While the lag is at most a few hours when the storm is placed in very strong (15 m s^{-1}) shear, storms in weaker shears experience much longer lag times, with the 5 m s^{-1} shear case showing no signs of weakening until more than 36 h after the shear is applied. These lags suggest that the storm intensity is to some degree predictable from observations of large-scale shear changes. In all cases both the development of the asymmetries in core structure and the subsequent weakening of the storm occur before any resolvable tilt of the storm's vertical axis occurs.

It is hypothesized that the weakening of the storm occurs via the following sequence of events: First, the shear causes the structure of the eyewall region to become highly asymmetric throughout the depth of the storm. Second, the asymmetries in the upper troposphere, where the storm circulation is weaker, become sufficiently strong that air with high values of potential vorticity and equivalent potential temperature are mixed outward rather than into the eye. This allows the shear to ventilate the eye resulting in a loss of the warm core at upper levels, which causes the central pressure to rise, weakening the entire storm. The maximum potential vorticity becomes concentrated in saturated portions of the eyewall cloud aloft rather than in the eye. Third, the asymmetric features at upper levels are advected by the shear, causing the upper portions of the vortex to tilt approximately downshear. The storm weakens from the top down, reaching an approximate steady-state intensity when the ventilated layer can descend no farther due to the increasing strength and stability of the vortex at lower levels.

1. Introduction

a. Overview

Tropical cyclones, called hurricanes in the Atlantic and northeast Pacific basins, are the most dangerous individual weather systems on Earth. The core of a mature tropical cyclone is an intense vortex with rotational winds that can approach 100 m s^{-1} within the eyewall cloud region surrounding the eye. Intense rainfall usually occurs within all or portions of the eyewall as well as in the spiral rainbands. Individual storms have killed as many as 300 000 persons and have caused property damage of at least $25 billion, yet some storms cause relatively little damage or loss of life, and even highly destructive storms often exhibit extremely small-scale variations in their damage patterns. As global population and wealth have become ever more concentrated along vulnerable coastlines, interest has grown in discovering the processes that govern the intensities and core structures of tropical cyclones and how to predict these quantities. This study examines one aspect of this problem—the effects of large-scale vertical wind shear upon the structure and intensity of tropical cyclones—using a series of numerical simulations of storms in idealized environments.

There have been many studies of the mean, quasi-steady structures of mature hurricanes (e.g., the recent review by Willoughby 1995). Some features of their

* Current affiliation: Department of Meteorology, U.S. Naval Postgraduate School, Monterey, California.

Corresponding author address: William M. Frank, Department of Meteorology, The Pennsylvania State University, University Park, PA 16802.
E-mail: frank@ems.psu.edu

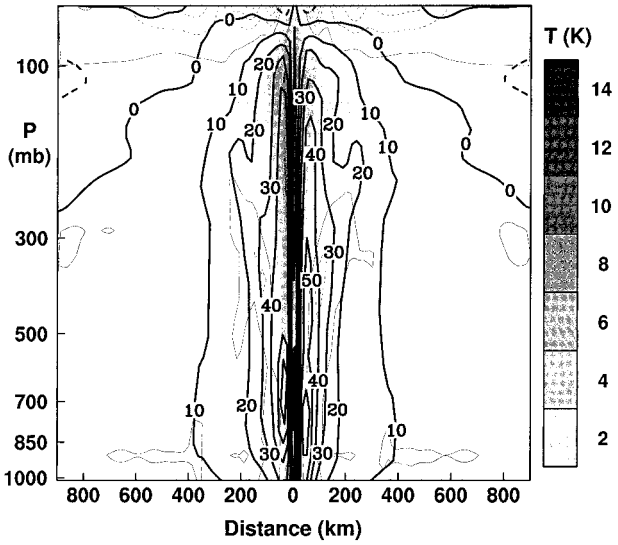

FIG. 1. Tangential winds at t = 48 h.

inner-core circulations are nearly axisymmetric, such as the pressure and temperature anomaly patterns. The tangential wind field is predominantly axisymmetric in the eyewall region, but it usually exhibits a significant degree of wavenumber one asymmetry as well. In contrast, the distributions of rainfall, convection, and radial winds can vary dramatically from nearly symmetric (usually observed only in very intense storms) to highly asymmetric. The degree of asymmetry in hurricane cores is neither well documented nor well understood, yet understanding the distribution of winds and rain in hurricanes is vital to both forecasting and understanding these dangerous storms.

Because of the first-order axisymmetry of the rotational winds and pressure field, several aspects of the storms can be described using axisymmetric conceptual models. Important examples include the basic wind pressure balance, the vertical structure of the warm-core vortex, and the basic energetics, including the interaction with the sea surface. Axisymmetric energetic arguments have also been used to estimate the maximum potential intensity (MPI) that a hurricane can achieve within an environment with a given thermodynamic structure [largely related to the sea surface temperature, the depth of the troposphere, and the vertical stability of the large-scale environment, Emanuel (1988) and Holland (1997)].

It is noteworthy that relatively few tropical cyclones seem to reach their MPI as defined above (Emanuel 1988) except perhaps during decaying stages when the storm is moving over relatively cold water. Those that do approach their MPI over tropical waters generally exhibit unusually symmetric core structures. Several explanations have been offered to explain the tendency for storms to remain well below their estimated MPIs, most of which focus into one of two areas. The first involves reductions of the energy flux from the ocean to the storm due to a combination of interaction with the ocean mixed layer (cooling the surface water) and processes that affect the character of the near-surface layer (e.g., sea spray). Emanuel (1999) used a simple coupled atmosphere–ocean model to show that the intensities of Atlantic hurricanes may persist closer to their modified MPI values (when ocean mixed layer cooling is taken into account) and, hence, may be more strongly governed by this thermodynamic limitation than is generally believed.

The second area involves arguments of the effects of asymmetries in the core structure upon storm intensity, and this latter area is the one addressed here. Virtually every tropical cyclone observed in nature has some obvious, significant asymmetries in its rainwater, vertical velocity, and wind patterns within the intense inner core. There are also large asymmetries in the rainbands and in the upper-level outflow anticyclone (outside the extreme inner core). What causes these asymmetries, and how might they prevent the storm from realizing its MPI?

Recent modeling studies of tropical cyclone–like vortices in idealized environments (described below) indicate that even modest amounts of vertical wind shear in the core region of a tropical cyclone can have strong effects on the asymmetric structure of the eyewall region, where the strongest winds and heaviest rains occur (e.g., Frank and Ritchie 1999; Frank 1998; Drury and Evans 1998; Bender 1997; Jones 1995). In general, these studies showed that the first-order effect of simple vertical shear profiles is to induce a wavenumber one asymmetry in the eyewall structure. Other studies have indicated that the movement of a hurricane in mean zonal flow results in asymmetries in the core structure that can affect intensity. Shapiro (1983) showed that a moving storm develops asymmetries in the patterns of frictional convergence within the boundary layer, which in turn induces asymmetries in the upward motion and rainfall patterns. Peng et al. (1999) simulated hurricanes in mean zonal flow and concluded that the resulting asymmetries reduced the intensity of the storms by interfering with the coupling between the regions of convergence and maximum surface fluxes in the boundary layer. Frank and Ritchie (1999) found that both shear and frictional processes produced asymmetries in dry and moist simulations, but the shear effects appeared to be stronger than frictional effects within the range of values they examined.

The present paper investigates the effects of shear on the inner-core structures and intensities of simulated tropical cyclones through a series of numerical simulations of idealized hurricane-like vortices subjected to different types of shear. The goal is to determine what types of asymmetries are caused by the shear and how they affect storm structure and intensity with time.

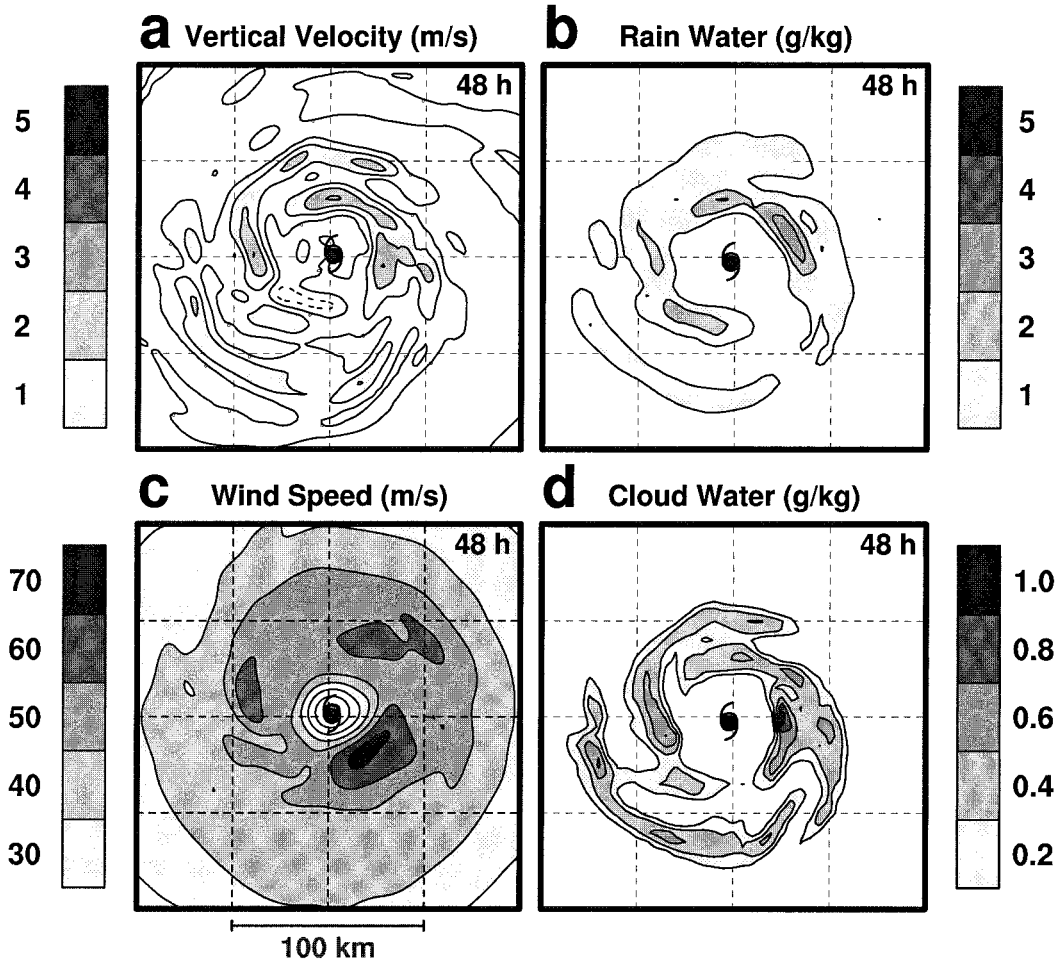

FIG. 2. Plan views of 700-mb vertical velocity (m s^{-1}), rainwater (g kg^{-1}), wind speed (m s^{-1}), and cloud water (g kg^{-1}) at $t = 48$ h. Each panel shows an area that is 200 km $\times$ 200 km. Dashed contours denote negative values.

b. Background

There is ample observational evidence that large-scale vertical shear has a generally negative impact on the formation of tropical cyclones (Gray 1968, 1979; Tuleya and Kurihara 1981). McBride and Zehr (1981) noted that developing tropical cyclones often have large vertical shear near the incipient storm center, but the shear is very weak over the core of the storm. While mature cyclones are thought to be more resistant to vertical shear than are forming storms, unidirectional shear in the core region has long been considered to have a negative effect on the intensity of even intense storms. The current hurricane intensity forecast system used at the National Hurricane Center of the National Oceanographic and Atmospheric Administration uses vertical shear as one of their statistical predictors (DeMaria and Kaplan 1994, 1999). Their research suggests that when vertical shear of approximately 8 m s^{-1} affects the core of hurricanes, it tends to cause the storm to weaken (J. Kaplan 2000, personal communication). Zehr (1992) has found that Pacific hurricanes generally do not form if the vertical shear between the 200- and 850-mb levels is greater than about 10 m s^{-1}. Several other observational studies have explored the relationships between vertical wind shear and the distribution of convection in the eyewall region, generally showing that the maximum rainfall tends to occur on the left side of the shear vector, looking downshear (e.g., Marks et al. 1992; Franklin et al. 1993).

How vertical shear affects the core and intensity of a mature hurricane remains an open question. Early studies, such as Gray (1968), hypothesized that the shear advected the warm upper-level air out of the center of the eye, raising the pressures at lower levels. DeMaria (1996) hypothesized that the shear caused the storms to tilt downshear. He argued that as the flow responds to imbalances in the vortex forced by the shear, the temperature anomaly in the center would increase at middle levels, and that this might inhibit convection in the core, thereby weakening the storm.

Jones (1995) performed simulations of tropical cyclone–like vortices in a dry model and found that the

shear caused the dry vortices to tilt downshear and to develop a wavenumber one asymmetry in the resulting vertical motion pattern. In her dry simulations the vortices went through a two-stage process resulting in maximum upward motion downshear right (looking downshear) of the center, with maximum forced subsidence occurring to the upshear left. Briefly, the tilt of the initially balanced vortex caused a direct dynamic response with weak upward (downward) motion downshear (upshear) of the center. This vertical motion tilted the isentropic surfaces causing a cold (warm) anomaly on the downshear (upshear) side. The primary circulation of the vortex then followed these tilted isentropic surfaces and dominated the overall vertical motion field, producing the maximum ascent on the downshear-right side.

Bender (1997) performed simulations of a tropical cyclone in vertical shear using the Geophysical Fluid Dynamics Laboratory (GFDL) model. His simulations were performed on both beta planes and f planes. Bender found that the vertical shear produced asymmetries in the eyewall structure, and he attributed these asymmetries to effects on the vorticity field caused by the asymmetric flow relative to the moving vortex. He found that the action of the winds on the vorticity field caused forced uplifting at lower levels, and that this uplifting tended to organize the convection and thus the rainfall in the eyewall into preferred patterns. In general, the convection appeared to favor the side to the left of the shear, though the maximum accumulated rainfall tended to occur on the upshear side of the storm.

Frank and Ritchie (1997, 1999) performed a series of numerical simulations of idealized tropical cyclones using the Pennsylvania State University–National Center for Atmospheric Research fifth-generation Mesoscale Model (MM5), which is a nonhydrostatic, three-dimensional model that includes both parameterized and explicitly resolved moist processes. They compared dry and moist simulations with similar initial conditions to examine the behavior of a sheared vortex when latent heating was allowed to occur. Their simulations were performed on an f plane to simplify the relationship between the imposed domain-average shear and the shear affecting the storm's inner core, and they examined only weak values of shear (3 m s^{-1}). They found that the latent heating in the eyewall region resulted in stronger vertical coupling of the storm than occurs in dry simulations, greatly reducing the tilt of the vortex. Nonetheless, their storms tended to produce a persistent wavenumber one asymmetry in the distribution of convection and rainfall, with both quantities being maximum on the left side of the shear vector. They noted that early in their simulations, when dry processes and parameterized convection dominated the simulation, the vortex behaved like the dry vortices of Jones (1995), producing maximum uplifting and convection in the downshear-right quadrant. However, as soon as the eyewall began to saturate, with the model's explicit moisture scheme becoming active, the convection tended to shift to the downshear-left quadrant. They attributed this to a destruction of the downshear cold anomaly of the dry runs due to resolvable moist ascent of slightly unstable air. This eliminated the adiabatic lifting mechanism evident in dry runs.

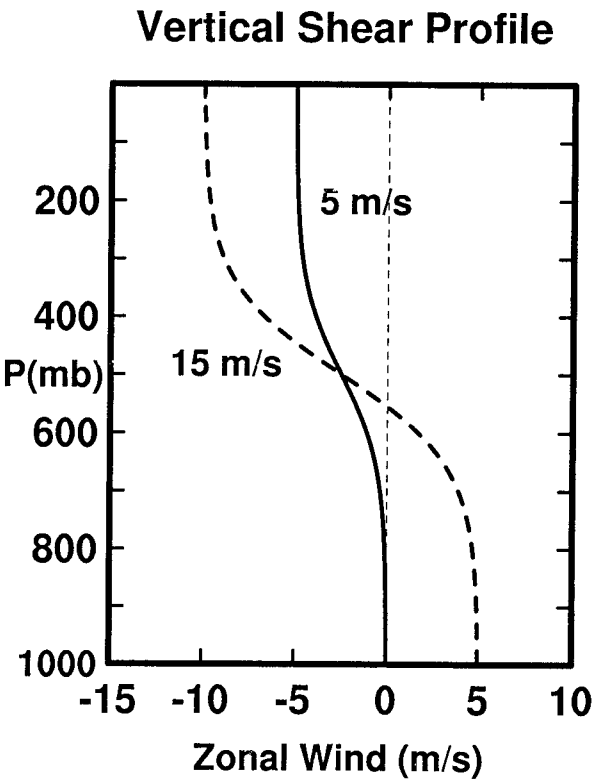

FIG. 3. The vertical wind profiles used in the sheared cases, normalized to the depth of the storm (m s^{-1}).

The dominant process in the moist runs appeared to be a result of the vorticity advection by the shear, which produced upper-level divergence and hence lower-level convergence downshear of the center. The ascending air rose in a cyclonic spiral on the left side of the shear vector, producing maximum latent heat release and rainfall on that side, with the rainfall maximum lagging the convective maximum by 45° or more. This rainfall pattern is in agreement with observations, as noted above.

The simulations by Frank and Ritchie (1999) were performed at a relatively coarse grid resolution of 15 km, and the cumulus parameterization scheme was used simultaneously with the explicit moisture scheme. They concluded that in order to pursue further studies of the effects of core on the core of a mature cyclone, it would be necessary to eliminate the cumulus parameterization and to obtain higher resolution of the eye and eyewall region, in part to examine the structure of the asymmetries that develop there. In the current study, the grid mesh is reduced to 5 km and the convective parameterization is turned off so that the convection in the core

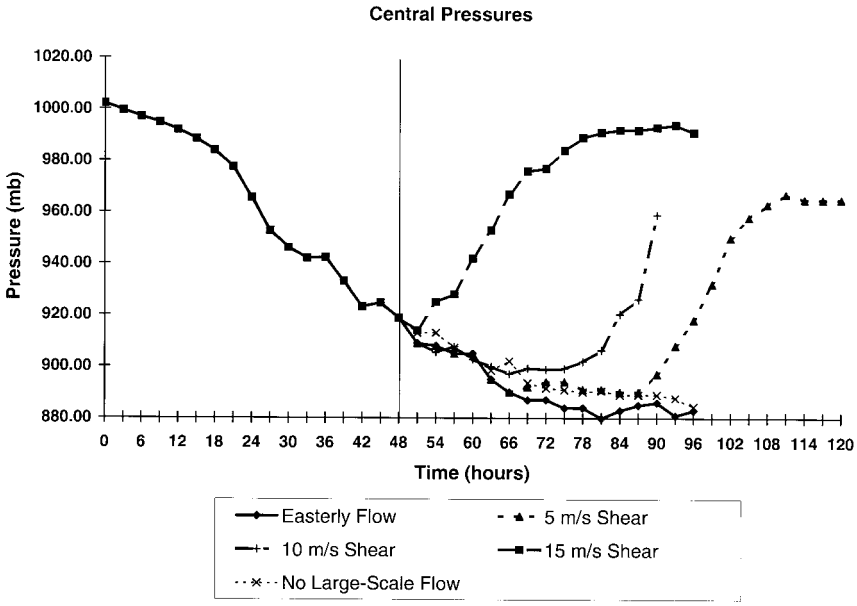

FIG. 4. Time series of minimum central pressures for the cases with constant easterly flow of 3.5, 5, 10, and 15 m s^{-1} shear, and no large-scale flow. The vertical line at $t = 48$ h is shown to mark the time at which the environmental fields are changed to introduce the shear or zonal flow.

is produced solely by the model's explicit moisture scheme.

2. Methodology

A series of numerical simulations are performed that simulate the effects of different types and magnitudes of vertical wind shear upon a mature tropical cyclone. Idealized initial conditions are used to simplify the large-scale fields and to facilitate isolating the cause and effect relationships.

The model is the MM5, and its configuration is similar to that described in Frank and Ritchie (1999) except for the addition of a third, finer mesh; the use of a different boundary layer scheme; and the use of fully explicit representation of moist convective processes rather than mixed explicit/parameterized convection. Briefly, the mesh domains are all square. The outer domain is 5400 km in each dimension with a 45-km mesh, the second domain is 1800 km with a 15-km mesh, and the finest mesh is 5 km over a fixed domain of 600 km. There are 20 vertical sigma levels. The model top is 50 mb, and a radiative boundary condition is used at the top of the model. Simulations are performed on an f plane valid at 15°N. The choice of an f plane was made to prevent the complications arising from interactions between the storm flow and the planetary meridional absolute vorticity gradient. Such interactions significantly alter the mean flow in the storm's core region (see, e.g., Bender 1997). While such interactions are important in nature, they complicate analysis of the effects of shear on the vortex since the induced circulation features vary significantly with the size and intensity of the storm, and the shear varies with radius. Use of f-plane symmetry ensures that the shear affecting the inner core region is very similar to that imposed upon the entire domain. We will extend our research to include simulations on a beta plane in the near future.

Boundary layer processes are determined from the level-2.5 turbulent kinetic energy scheme of Shafran et al. (2000). During the initial spinup of the storm the model uses both a simple cumulus parameterization (Betts and Miller 1986) and the explicit moisture scheme of Dudhia (1989). As described below, once the model begins to produce saturated conditions in the eyewall region of the developing storm, the cumulus parameterization is switched off, and the remainder of each simulation is performed using only the explicit moisture scheme. In the simple ice scheme all condensate is assumed to be frozen at temperatures below 0°C, and there is a single ice type (snow). None of the simulations described below included radiative processes. Simulations have been performed with and without interactive radiation, but for the types of runs described here, it is preferable to avoid radiative processes in order to retard the growth of convection on the outer grid meshes. Since the domain size is quite large, very little mean stabilization occurs.

The sea surface temperature (SST) is fixed at a uniform value of 28.5°C. The initial thermodynamic sounding is taken from the prestorm cloud cluster composite of McBride and Zehr (1981), which was determined from rawinsonde data in the northwest Pacific. When either mean zonal flow or mean vertical shear is added

to the domain, the sounding at the center of the domain is kept constant, and the temperatures are adjusted to achieve geostrophic balance. The types of shear imposed are described later. In most cases the mean winds and shears are imposed such that the storm tends to move along a track that has approximately constant vertical stability.

All of the simulations begin with the same initial, baroclinic vortex, which is axisymmetric with maximum winds of 15 m s^{-1} at a radius of 135 km—equivalent to a strong tropical depression. This is the same initial vortex that was used in Frank and Ritchie (1999). There is a broad anticyclone aloft, and the fields are in gradient balance. At the time of initialization there are no large-scale winds in the domain, and only the two coarser grid meshes are used. The storm quickly intensifies, and by 36 h the eyewall region has begun to saturate. At that time the cumulus parameterization is turned off, and the model fields are interpolated to the fine mesh (5 km), which is used for the duration of the run. At $t = 48$ h the storm has developed into an intense tropical cyclone (Fig. 1) with a central pressure of about 920 mb. The mean core wind and pressure structure is largely axisymmetric, though fields such as cloud water, rainwater, and vertical velocity show temporary asymmetries resulting from the cellular nature of eyewall convection (Fig. 2). However, none of the fields show preferred regions of occurrence when averaged over time.

At this time ($t = 48$ h) the large-scale wind fields, consisting of either mean zonal flow and/or vertically sheared flow, are imposed. The imposed winds are zonal and are horizontally uniform at each sigma level. The pressure and temperature fields are adjusted so that the large-scale winds are in geostrophic balance. This is done by adding positive (negative) temperature anomalies north (south) of the central latitude of the domain so that the vertical stability along the central latitude is unchanged. In this study all of the storms move almost directly eastward (by design), so they do not move into regions of increased or decreased large-scale stability. While there are some slight imbalances in the initial flow fields in the vicinity of the storm when the shear is imposed, their effect on the simulated storms is brief and temporary. As described below, the simulated storms continue their intensification unabated, and the asymmetries that develop after the shear is imposed are persistent, indicating that they are quasi-balanced rather than transient phenomena. One possible exception is the 15 m s^{-1} shear case, which dissipates rapidly. It is possible that the shock of adding the shear suddenly accelerates the demise of the storm in this case, and the results should be interpreted in that light. Finally, adding the north–south temperature gradients creates a weak meridional gradient of background potential vorticity (PV) and, hence, a weak beta effect. Diagnostic analysis of the simulations indicated that the effects of the storm's interaction with this weak PV gradient had no significant effect on the results.

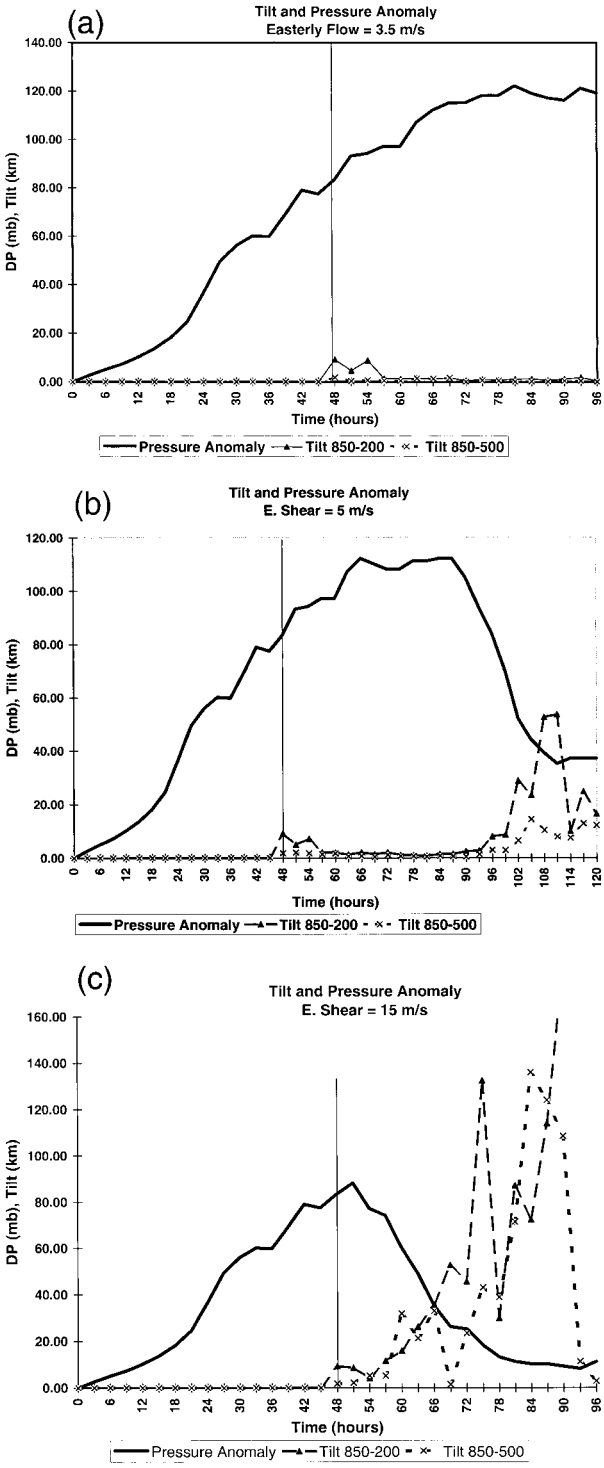

FIG. 5. Time series of the storm pressure anomaly (difference between the minimum central pressure and the initial vortex central pressure of 1002.2 mb), the tilt of the storm center between 850 and 500 mb (km), and the tilt between 850 and 200 mb (km) for the (a) 3.5, (b) 5, and (c) 15 m s^{-1} shear cases. The vertical lines at $t = 48$ h indicate the time at which the environmental flow is altered.

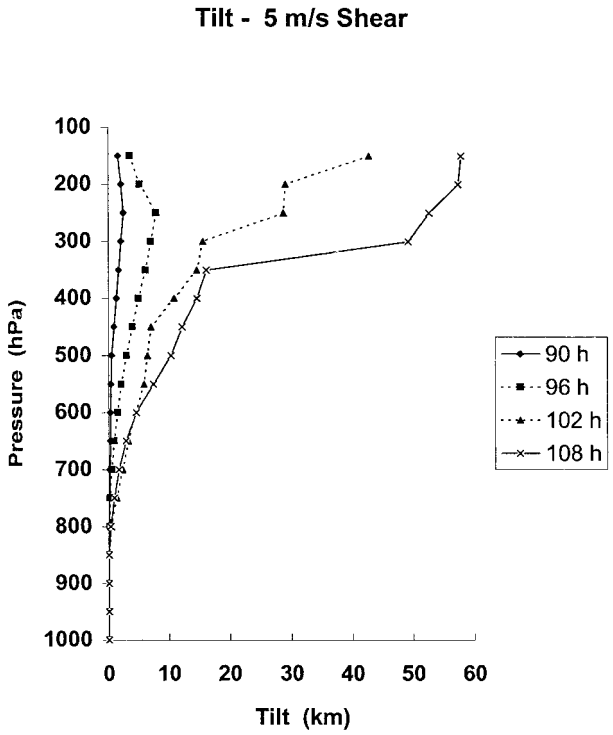

FIG. 6. Vertical profiles of the axis tilt (total displacement of vortex center from surface location, km) at different times for the 5 m s^{-1} shear case.

Five simulations are discussed in this paper. One has no large-scale flow, one has uniform easterly flow of 3.5 m s^{-1} at all levels, and three have vertical shears of 5, 10, and 15 m s^{-1}, respectively. The shear profiles are unidirectional and easterly with the shapes shown in Fig. 3. The 10 m s^{-1} shear profile (not shown) is the same shape as the 5 m s^{-1} profile but with the values multiplied by two. This is the same profile used in Frank and Ritchie (1999). Effects of cross-track and multidirectional shear are currently being studied and will be reported upon in a future paper. In these runs the storm tracks approximately due westward.

Most of the runs continue until $t = 96$ h, 48 h after the environmental flow is added. One continues to 120 h, and one is terminated after 87 h due to the storm moving too close to the edge of the fine mesh domain.

3. Results

a. Relationships between shear, vortex tilt, and storm intensity

Figure 4 shows the evolution of the central pressures for all of the simulations. The central pressure is felt to be a better indicator of the overall indicator of the intensity than is the local wind speed maximum, so the discussion will emphasize changes in that pressure. All simulations are identical through 48 h, when the environmental flows are imposed. Based on the MPI arguments of Emanuel (1988), all of the storms in this study would have an estimated minimum central pressure of about 880 mb, based on the fixed SST of 28.5°C and the initial sounding. In nature storms rarely achieve this intensity, but it must be remembered that these simulations are performed without the inhibiting factors of interactions with the sea surface, including effects of upwelling, spray, waves, and possible limitations on the air–sea energy fluxes at high wind speeds. The 10 m s^{-1} run is terminated at $t = 87$ h since the storm is then approaching the edge of the fine mesh domain. (The 15 m s^{-1} run moves more slowly and does not approach the edge of the inner domain within 96 h.)

The no-flow run and the easterly flow run, which also has no shear, are the most intense simulations. The easterly flow storm becomes slightly more intense than the zero-flow case. As will be shown below, the easterly flow run develops significant asymmetries in eyewall structure, but it nonetheless becomes an extremely intense hurricane, approaching central pressures of 880 mb and remaining near that intensity through the end of the simulation at 96 h. The reason that the mean easterly flow produces a stronger storm than the zero-flow case is that the boundary layer evolution is more favorable for the moving storm. In the zero-flow case the storm remains almost stationary, and the boundary layer in the core is cooled somewhat by evaporation of rainfall and resolvable-scale downdrafts. These processes slightly reduce the equivalent potential temperature (θ_e) of the core air that rises in the eyewall cloud. In contrast, the easterly flow case moves westward at a steady pace, resulting in advection of undisturbed air into the eyewall region on the west side where it develops higher values of θ_e.

All of the easterly shear cases show significant weakening of the storm. When 15 m s^{-1} of shear is added to the domain, the storm begins weakening after about 3 h. Within about 30 h ($t = 78$ h of the simulation) the storm has weakened to tropical storm intensity (maximum winds between 18 and 32 m s^{-1}), and it remains a loosely organized tropical storm through the end of the run at 96 h. The storm with 10 m s^{-1} of easterly shear continues to intensify for 18–24 h, then begins to weaken. The 5 m s^{-1} easterly shear run continues to intensify until about 84 h, then weakens relatively rapidly until it levels off as a moderate hurricane with a central pressure of just over 960 mb around 108 h.

In order to interpret interactions between vertical shear and storm intensity, it is necessary to examine the effect of the shear on the vertical orientation of the vortex. In dry simulations (e.g., Jones 1995; Frank and Ritchie 1999) there is little vertical coupling in the storm due to the very weak vertical motions and resulting weak vertical fluxes of momentum. As a result, the vortices develop considerable tilt of the axis of rotation, and for baroclinic vortices this increases approximately linearly with time (Frank and Ritchie 1999). If the axis

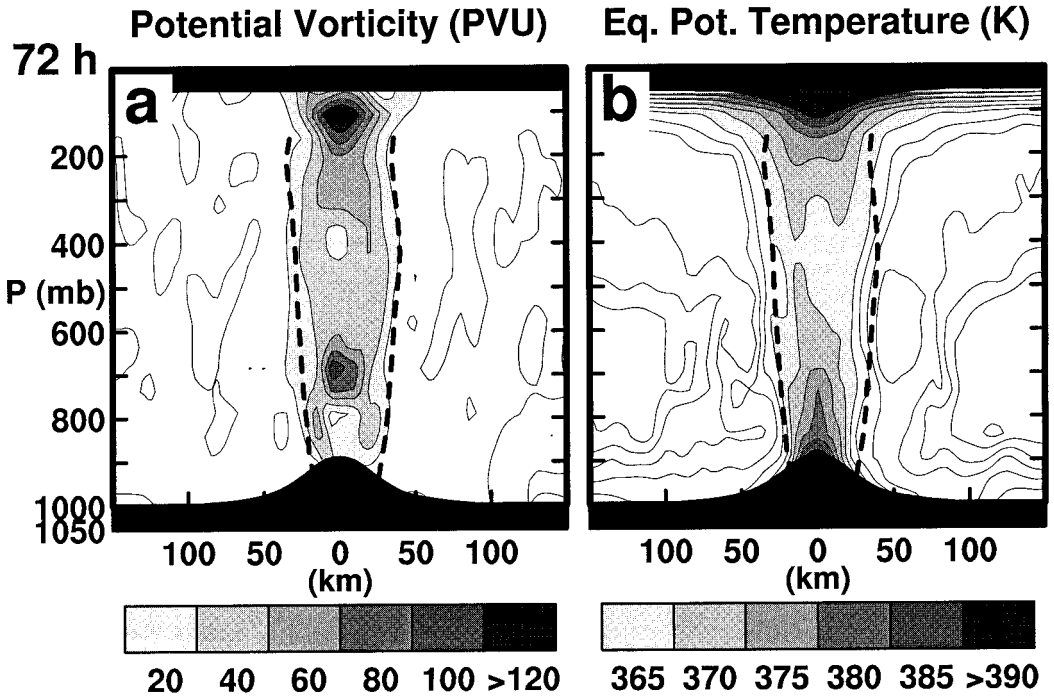

FIG. 7. Vertical cross sections of potential vorticity (PVU) and equivalent potential temperature (K) at $t = 72$ h for the case with no large-scale flow. The dashed vertical lines indicate the location of the radius of maximum winds.

of rotation at upper levels is displaced relative to that at lower levels by distances on the order of the radius of maximum winds (RMW) or greater, at least three important effects on the core structure may occur: The central pressure of the vortex may rise due to simple hydrostatic arguments. Further, the upward (downward) projection of the PV anomalies at lower (upper) levels can affect the motion of the vortex, alter the advection of PV and other quantities at other vertical levels, and induce vertical motion—typically upward motion in the direction of tilt and subsidence on the other side, which can affect the organization of convection. Finally, the relative displacement of the upper-level vortex relative to the low-level vortex tends to cause strong changes in the magnitude and direction of the vertical shear in the eyewall (i.e., the strong rotational flow near the RMW at upper levels may cross the flow at lower levels at nearly perpendicular angles, while the two flows tend to be parallel in a vertically aligned storm).

To examine the tilt of the storm's vertical axis, time series of the surface pressure anomaly from the initial surface pressure are compared to time series of the total horizontal distances between the estimated vortex center at 850 mb and the centers at 500 and 250 mb (Fig. 5). The vortex positions are estimated from the position of the interpolated minimum pressure (largest negative pressure anomaly) at each sigma level. The minimum pressure location varies slightly more smoothly than do other measures of the vortex center, such as the vorticity maximum or the interpolated center of circulation. When the pressure minimum is no longer distinct, no tilt is calculated. It should be kept in mind that due to the 5-km grid used in these simulations, tilts of a few kilometers or less are not resolved, and hence they should merely be regarded as being less than one grid interval.

Figures 5a–c illustrate the relationship between storm intensity and vortex tilt for three cases (mean easterly flow, 5 m s^{-1} easterly shear, and 15 m s^{-1} easterly shear). In the case with uniform easterly flow and no imposed shear, the vortex does not tilt at any time except during a brief adjustment period between $t = 48$–60 h, immediately after the easterly flow is added. The storm continues deepening after the mean zonal flow is added, as noted above. The 5 m s^{-1} shear case evolves differently. As in the nonsheared case there is a small, brief tilt of the vortex associated with the addition of the large-scale flow. The storm quickly overcomes this and continues to intensify, and it becomes vertically aligned once again by $t = 60$ h. However, this case begins to fill between $t = 87$–90 h, with the central pressure rising 7 mb during that 3-h interval and rising monotonically until $t = 111$ h, when it levels off at about 965 mb. Neither the 850–500-mb nor the 850–250-mb estimated tilt exceeds 3 km (which is below the grid resolution) at any time through 93 h. The storm weakens by 19 mb between $t = 87$–93 h without any significant tilt of the vortex. At about $t = 96$ h the vortex begins to tilt generally toward the southwest. At no time does the 850–500-mb tilt exceed 14 km, which is less than the di-

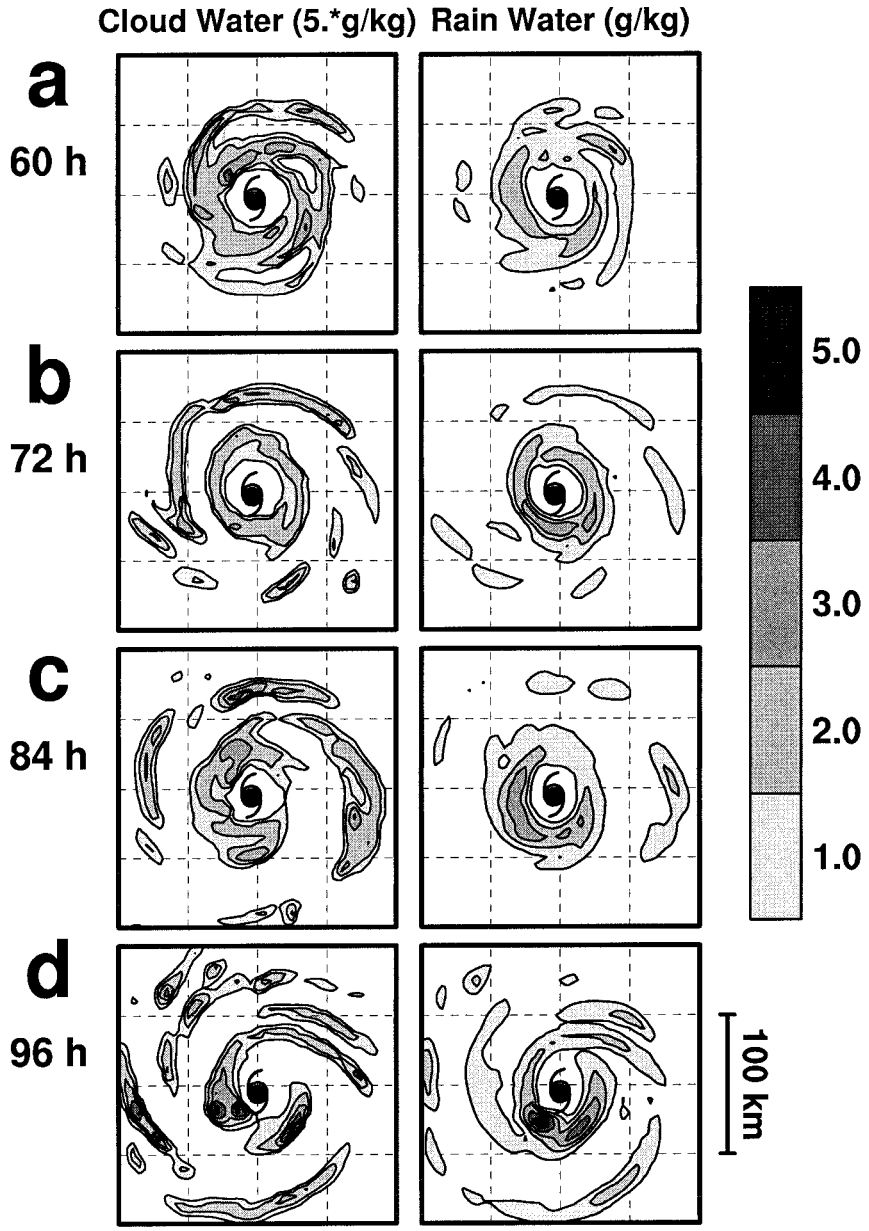

FIG. 8. Plan views of cloud water and rainwater (g kg^{-1}) for the 3.5 m s^{-1} zonal flow run at 700 mb, and at t = 60, 72, 84, and 96 h. Each panel shows an area that is 200 km × 200 km.

ameter of the eyewall cloud and of the RMW (which is typically about 20–30 km at the more intense stages), and given the generally flat distributions of temperature and pressure within the eye, the warm anomaly can be considered as being close to vertical in the lower half of the troposphere. However, the upper levels of the storm behave quite differently.

The major changes induced by the shear begin aloft. Between about t = 99 and 102 h the extreme upper levels of the vortex begin losing their symmetric structure, and the features begin moving generally to the downshear left of the low-level center. Details of these structural changes are discussed in the next section, but one net effect is that within the upper layers the circulation develops a strong tilt, generally toward the southwest. The magnitude of the tilt is such that the apparent center of circulation in the upper layers is displaced from the low-level center by a distance that is comparable to the RMW at 950 mb (which varies between 26 and 30 km throughout this case). The layer of strong tilt descends with time (Fig. 6) as the upper layers of the storm become increasingly asymmetric and less coupled to the low-level vortex.

When 15 m s^{-1} of shear is imposed, the storm in-

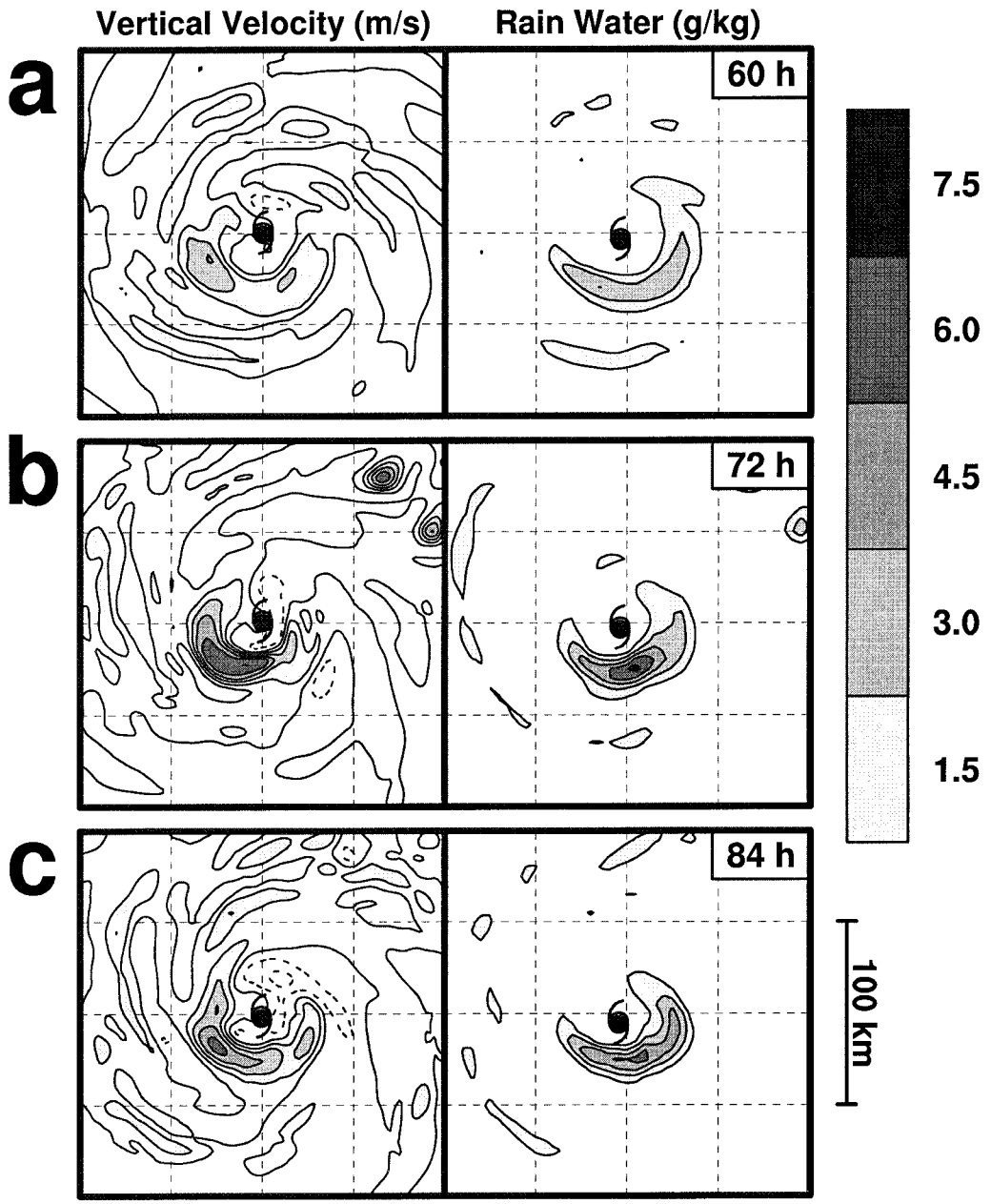

FIG. 9. (a)–(f) Plan views of vertical velocity (m s^{-1}) and rainwater (g kg^{-1}) for the 5 m s^{-1} shear run at 700 mb, at t = 60, 72, 84, 96, 108, and 120 h for a 200 km × 200 km area. Dashed contours denote negative values.

tensifies only during the next 3 h and then fills steadily until about t = 84 h, when it levels off between 991 and 994 mb. As in the 5 m s^{-1} shear simulation the storm remains vertically aligned through t = 54 h, but by t = 57 h the storm becomes asymmetric at upper levels, and the storm begins to tilt and weaken. By about t = 72 h the storm has weakened to tropical storm intensity, and it persists as a loosely organized tropical storm, with central pressures around 990 mb, through the rest of the simulation. The large tilts indicated after t = 72 h result from the loss of a distinct vortex center in the upper levels and are not representative of true vortex tilt.

Summarizing, the imposed vertical wind shears had significant effects on the intensities of the simulated storms, weakening the storms in all cases. A shear of 15 m s^{-1} was sufficient to destroy the hurricane, weakening it to a loosely organized tropical storm very quickly, while shears of 10 m s^{-1} or less weakened the storm but did not reduce it below hurricane intensity within 24 h. Observational studies have indicated that there may be a threshold shear near 8–10 m s^{-1} at which

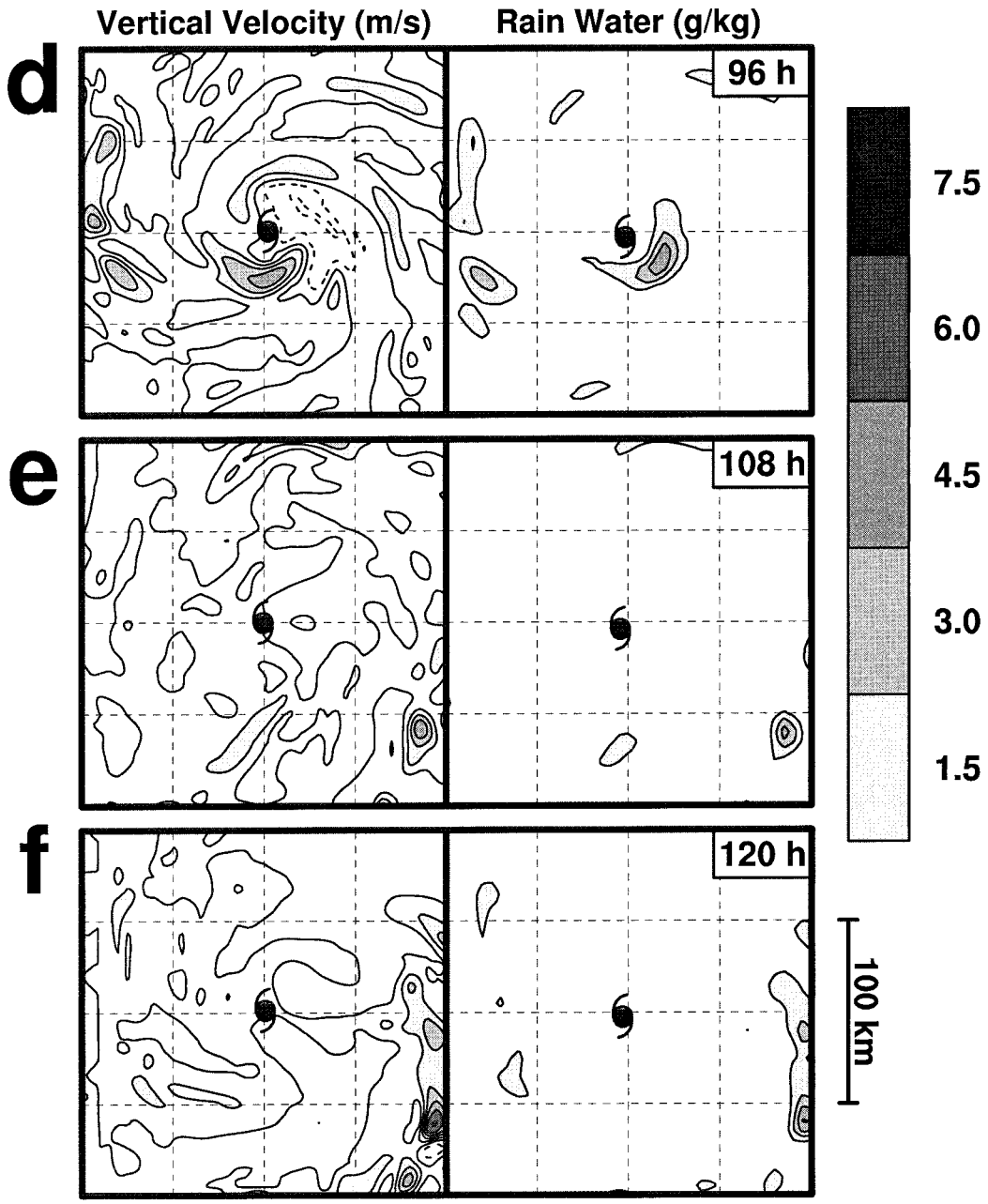

FIG. 9. (*Continued*)

major weakening of a storm would be expected to occur (DeMaria and Kaplan 1994; Zehr 1992; J. Kaplan 2000, personal communication). An interesting aspect of the shear simulations is that the weakening is not immediate in the storms with shears of 5–10 m s^{-1}. These storms continued to intensify for periods of up to 36 h before weakening occurred, though all of the shear runs became at least slightly weaker than the easterly flow run by the end of the first day after the shear was imposed. The processes causing the observed variations in storm intensity are discussed in the next section.

b. Shear effects on core structure

Hurricanes in nature are never fully symmetric, and neither are any of the simulated storms in this study. The zero-flow case is the most symmetric, as expected, but even this storm develops some asymmetries in the inner core cloud water and rainwater patterns similar to those shown in Fig. 2. The asymmetries in the eyewall cloud itself are relatively small and reflect primarily the cellular nature of convection, but there is obvious organization into spiral rainbands just outside the eyewall.

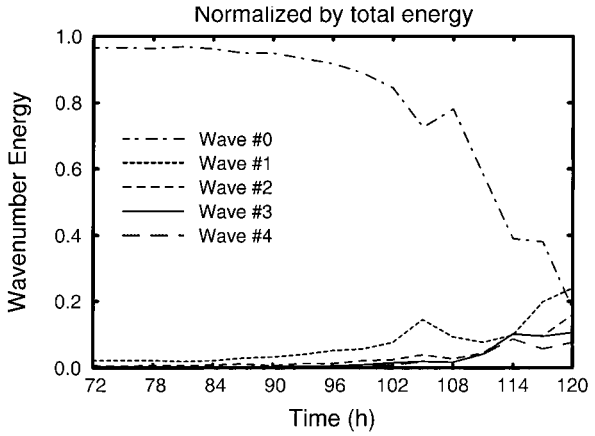

FIG. 10. Time series of Fourier components of the potential vorticity field for the region extending from the center to 270-km radius and from 900 to 200 mb.

In these figures and those that follow cloud water is generally indicative of saturated air and upward vertical motion. Since rainwater is a predicted variable, it is advected by air motions, has a fall velocity, and does not evaporate instantly when it is in unsaturated air. Maxima in rainwater tend to occur downstream from maxima in cloud water, while the latter tend to be coincident with regions of strong ascent.

It should be noted that each of the figures of storm structure shown below is based on output at a single time step. Bender (1997) has noted that in his studies using the GFDL hurricane model some features of eyewall asymmetries are sufficiently variable in time and space that they are clearer when the eyewall structure is averaged over longer time periods. However, such averaging also tends to obscure the spatial scales and magnitudes of smaller-scale features. In the present study we have chosen to display instantaneous images at regular time intervals in order to illustrate the structural features of the eyewall region more sharply than could be achieved in composites. While only selected figures are shown, we examined many such figures throughout the lifetime of each run to assess the persistence of major features in time and space. These attributes are discussed in the text. In general, the locations of individual updrafts and of rain and cloud water maxima vary in time but remain on one side of the eye through most of a simulation. The most spatially consistent asymmetric feature of the modeled eyewalls tends to be the relatively clear region (a distinct minimum in cloud and rainwater).

The zero-flow simulation maintains a compact, erect core, with maximum values of potential vorticity and equivalent potential temperature (θ_e) concentrated within the eye at all levels throughout the troposphere (e.g., Fig. 7). This is consistent with the steady and extreme intensity of the storm throughout the simulation.

An obvious question is, How does air with maximum values of θ_e and PV get into the eye, given that the highest θ_e values are generated at the surface and ascend in the eyewall cloud surrounding the eye, while the high PV values are generated within the saturated eyewall cloud? At least three mechanisms exist for concentrating vorticity at the center of a hurricane-like vortex in the lower and middle levels. Vorticity and/or PV can be generated in the eyewall cloud and other convective rainbands outside the eye and then merged into the central portion of the vortex by axisymmetrizing properties of the flow. This type of process was described in terms of vortex mergers by Ritchie and Holland (1997) and in terms of vortex Rossby wave behavior by Moeller and Montgomery (1999). This mechanism can both transport vorticity generated in rainbands outside the eyewall inward, and it can also transport vorticity from the eyewall into the eye itself. Second, vorticity/PV in the eyewall cloud can increase due to local generation, causing the eyewall to become barotropically unstable. This instability can produce vortex Rossby waves and possibly mesovortices, which can mix cyclonic vorticity inward and anticyclonic vorticity outward (Schubert et al. 1999). Finally, turbulent mixing can mix air with high cyclonic momentum into the eye, spinning up the flow there. Since the above processes can mix air from the eyewall cloud into the eye itself, they can transport air with high θ_e values inward as well. In the upper levels one must add the possibility of subsidence of air from the lower stratosphere or from the extreme upper portions of the troposphere near the eyewall to the above three mechanisms.

All of the above mechanisms may be acting to various degrees in the runs shown in this paper. Examination of the eyewall PV fields at many individual times shows that the eyewall develops asymmetries and changes shape in a manner much like the patterns shown in the studies of vortex Rossby waves (e.g., Moeller and Montgomery 1999). Such waves result in eyewall mesovortices at times. Diffusion represents an analogy (albeit a crude one) to horizontal turbulent transports at the edge of the eyewall. However, it is likely that the relative magnitudes of each process within the eye and eyewall region are not well simulated by the model due to the grid resolution used (5 km). Observations of eyewall mesovortices made using Doppler radar often show these eddies to be on the order of 1–5 km (e.g., Black and Marks 1991), below the resolution of the model, and horizontal diffusion is at best a very crude estimate of turbulent mixing when applied on a grid this large. We plan to perform similar simulations in the future using approximately 1-km grid meshes upon expansion of the available computer resources, and ultimately, the topic should be explored down to the grid meshes of large eddy simulations (tens of meters). For the present we will focus the discussion on the large-scale and hence better-resolved features of the simulations, and their relationships to the imposed environments, leaving the

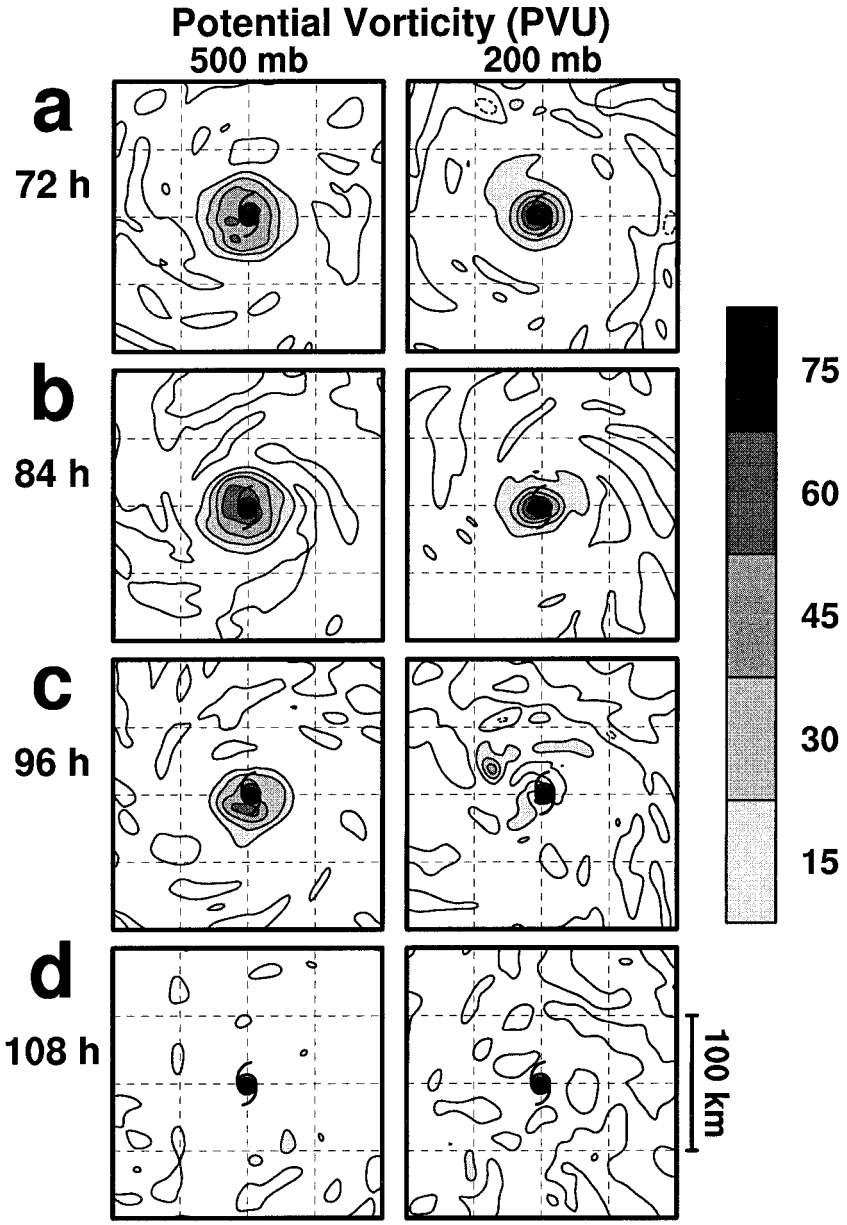

FIG. 11. Plan views of PV at 500 and 200 mb for the 5 m s^{-1} shear case, at t = 72, 90, 96, and 108 h for a 200 km × 200 km area.

more detailed physical diagnostic analyses of the nature of the eye–eyewall interactions until the next paper.

The easterly flow case, with no imposed vertical wind shear, is the most intense of the simulations, as noted previously. This storm tracks westward at 3.5 m s^{-1}, which is approximately the same direction and speed that the storm moves in the 5 m s^{-1} easterly shear run. Shapiro (1983) showed that the asymmetries in friction that occur in the boundary layer of a moving, otherwise symmetric vortex tend to cause a wavenumber one asymmetry in convergence. He found that the pattern varied slightly with storm speed, but for slow to moderate moving storms the maximum convergence occurred ahead and to the right of the storm center, looking down the track. Frank and Ritchie (1999) found very similar patterns in their dry simulations using MM5, and they noted that the convergence pattern was primarily evident below about 850 mb. This persistent asymmetry in low-level convergence forced by friction has long been assumed to influence the organization of vertical motion and convection within the eyewall region.

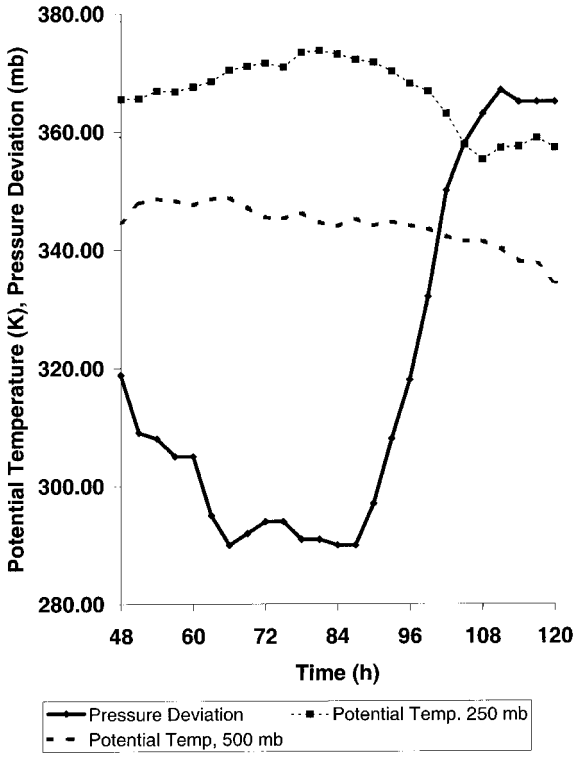

FIG. 12. Time series of maximum values of potential temperature at 200 mb and at 500 mb, along with the minimum surface pressure minus 600 mb, for the 5 m s^{-1} shear case.

Figure 8 shows the cloud water and rainwater patterns at 700 mb for the easterly flow run at t = 60, 72, 84, and 96 h. Cloud water is highly correlated with upward vertical velocity, as discussed earlier. These figures are illustrative of the typical patterns observed for this case. (In this run the 700-mb surface tends to be around 2 km above the surface in the inner core and thus intersects the eyewall convection at a low level.) At this level the cloud water pattern, and hence the upward vertical motion pattern, varies between periods that are almost axisymmetric (e.g., Figs. 8a,b) and other periods when they show more of a wavenumber one asymmetry, with maximum upward motion either ahead or to the left of the track (Figs. 8c,d). Overall, this case is more symmetric than the shear simulations, as expected. The frictional convergence pattern in the boundary layer causes a preference for convective cells to occur generally ahead of the storm relative to behind it, but this forcing is not strong enough to maintain a constant asymmetric pattern.

The rainwater patterns in Fig. 8 are more symmetric than are the updraft patterns. This is typical, since the rainwater at a given level consists of both hydrometeors within areas of active ascent and others that have fallen from higher levels. Further, rainwater tends to persist in time after the conditions that produced it have ceased to exist. In general, the maxima in rainwater concentrations occur roughly 45° downstream (counterclockwise) from the updraft and cloud water maxima in the eyewall, as was true in Frank and Ritchie (1999).

The 5 m s^{-1} easterly shear run develops clear wavenumber one asymmetries in the eyewall structure within a few hours of the time that the shear is imposed. By t = 54 h the low-level upward vertical velocity and rainwater in the eyewall have become concentrated in the southern (left of shear) portion of the eyewall (not shown), and this pattern persists throughout the first 48 h after the shear is added (Fig. 9). By t = 108 h, after the storm has undergone major weakening, the eyewall has become poorly defined (Figs. 9e,f).

The output from the 5 m s^{-1} shear run was subjected to Fourier decomposition of the potential vorticity field to analyze the wave energy in a region ranging from the center to 270-km radius and for the layer between 900 and 200 hPa. The results for wavenumber zero (symmetric) and for wavenumbers one through four are shown as time series in Fig. 10. As expected, most of the energy is in the symmetric mode until the storm begins to weaken, though the wavenumber one energy increases steadily. After about t = 87 h, when the storm fills, there is a steady growth in the wavenumber one energy and a corresponding decrease in energy of the symmetric mode. During this period the storm is becoming more asymmetric from the top down. None of the other wavenumbers show energy changes comparable to the wavenumber one mode until around t = 111–114 h, when the vortex structure has become much more irregular (discussed above). Thus, the storm weakening occurs in concurrence with the growth of wavenumber one asymmetry but is not well related to higher-order wavenumbers.

As noted above, the rapid filling that occurs in the 5 m s^{-1} shear run between about t = 87–96 h is not associated with a concurrent tilt of the vortex. However, the filling is concurrent with distinct changes in the PV pattern at upper levels. As the filling begins between about t = 87–90 h, the PV field at 200 mb is beginning to change from a symmetric pattern with a maximum in the eye to an asymmetric pattern with maxima in the eyewall cloud region, in this case north and west of the center (Fig. 11). By t = 96 h and thereafter the 200-mb PV maxima occur in bands and/or local maxima that are located at or outside the approximate radius of the eyewall at lower levels. These PV maxima are clearly not in the center of the vortex. During the period between t = 90 h and t = 102 h, the PV pattern at 500 mb continues to maintain a targetlike structure with maxima in the eye, but the magnitude of the PV decreases by more than a factor of 2. By t = 108 h there is no longer a discernable PV maximum at either 500 or 200 mb, though a weak one persists at 700 mb. For reasons discussed below, it appears that the PV is advected outward from the eye due to asymmetries in the circulation.

From examination of the results at all of the times

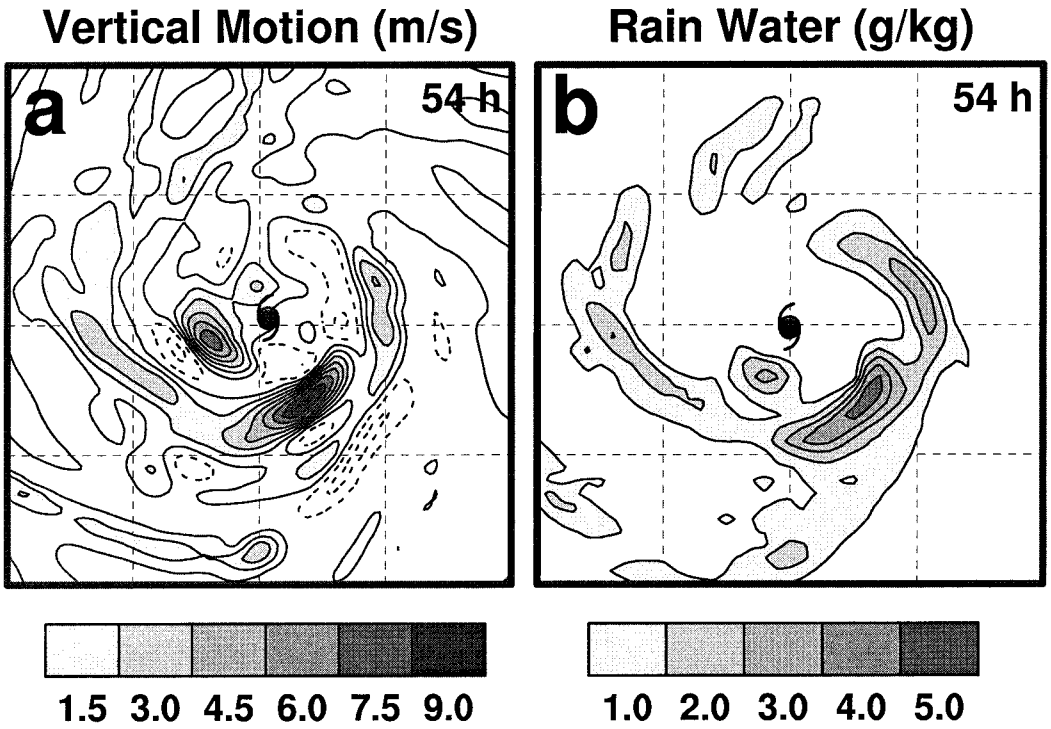

FIG. 13. Plan views of vertical motion (m s^{-1}) and rain water (g kg^{-1}) at 700 mb for the 15 m s^{-1} shear case at t = 54 h (200 km × 200 km area). Dashed lines denote negative values.

and levels, it is clear that the storm is weakening from the top down. The sequence of events is that the shear rapidly influences the structure of the vortex at all levels producing strong, persistent wavenumber one asymmetries in the patterns of eyewall vertical motion and related properties, such as cloud water and rainwater. At the upper levels, where the vortex is weakest, the vortex loses its symmetric structure with central maxima of PV and instead exhibits maxima of PV only within regions of active ascent in the eyewall itself. Concurrently, the temperature anomaly within the eye at upper levels weakens, raising the surface pressure of the storm and weakening the overall circulation. These changes in structure do not occur until 24–36 h after the shear is imposed for this case with relatively moderate shear (5 m s^{-1}). The asymmetries in the PV field and the eye–eyewall structure in general subsequently extend downward with time.

Figure 12 shows time series of the anomalies of the θ values at 500 mb and at 250 mb, along with the central pressure, for this case. (A constant value of 600 mb has been subtracted from the central pressures to aid in plotting.) The time series of θ at 250 mb shows a rapid drop associated with the ventilation of the eye at that level. This occurs in conjunction with the rapid rise in central surface pressure. In contrast, θ at 500 mb remains relatively steady through the period from 78 to 96 h despite the rapid rise in surface pressure between 87 and 96 h, showing that the warm-core structure dissipates aloft rather than in the middle levels. After 96 h there is a slow and steady decline in θ at 500 mb as the storm continues to weaken.

The results of the 15 m s^{-1} shear case are qualitatively similar to those of the 5 m s^{-1} case, though the changes occur much more rapidly. By t = 54 h, just 6 h after the shear is imposed, the storm is highly asymmetric (Fig. 13), and the PV pattern has changed from one with maximum values in the eye to an asymmetric pattern with maximum values in the eyewall cloud region even at levels as low as 700 mb (Fig. 14).

Figure 15 shows time series of several quantities for the three cases for the period from 48 to 96 h. These quantities are the minimum central pressure, the total rainfall during the previous 3 h, the maximum potential temperature (θ) at the 250-mb level, and the maximum θ_e at the surface. The rainfall was averaged over the region from 0- to 50-km radius to capture primarily rain in the eyewall cloud during stages when the storms had well-developed eyes rather than precipitation in the rainbands.

In the mean zonal flow case θ at 250 mb increases monotonically through most of the period shown, varying approximately inversely with the surface pressure, and the maximum value of θ always occurs within the eye, at or near the circulation center. This reflects the simple hydrostatic relationship between temperature anomaly and surface pressure for a vertically aligned vortex of approximately constant depth. Values of θ_e at

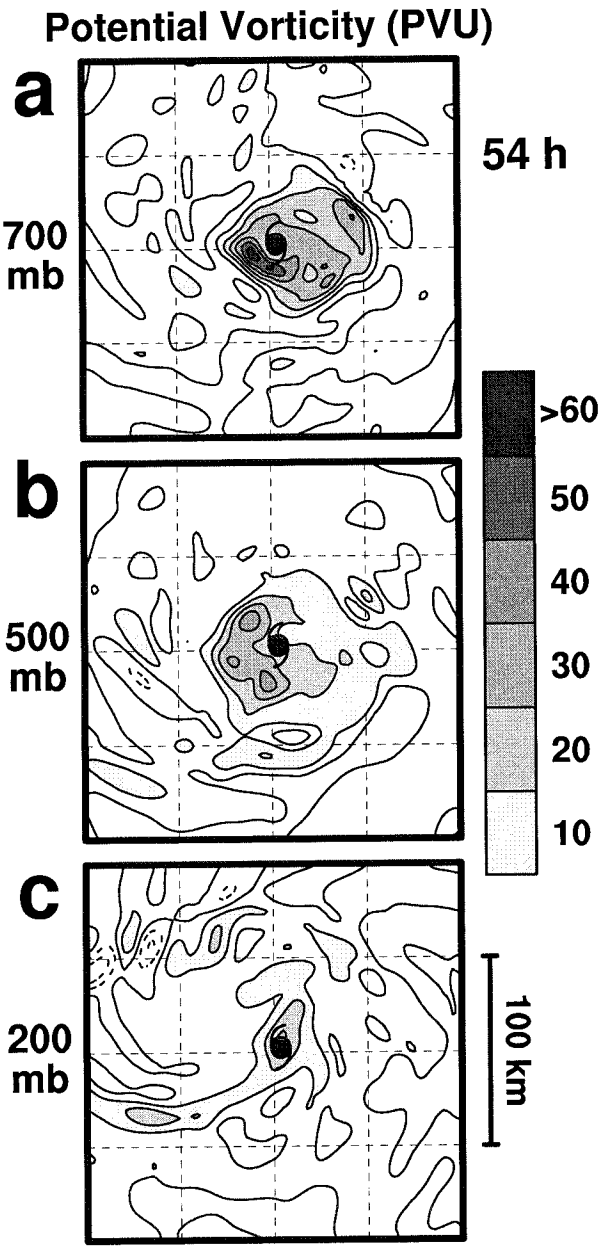

FIG. 14. Plan views of PV for the 15 m s^{-1} shear case at 700, 500, and 200 mb at t = 54 h (200 km × 200 km area). Dashed lines denote negative values.

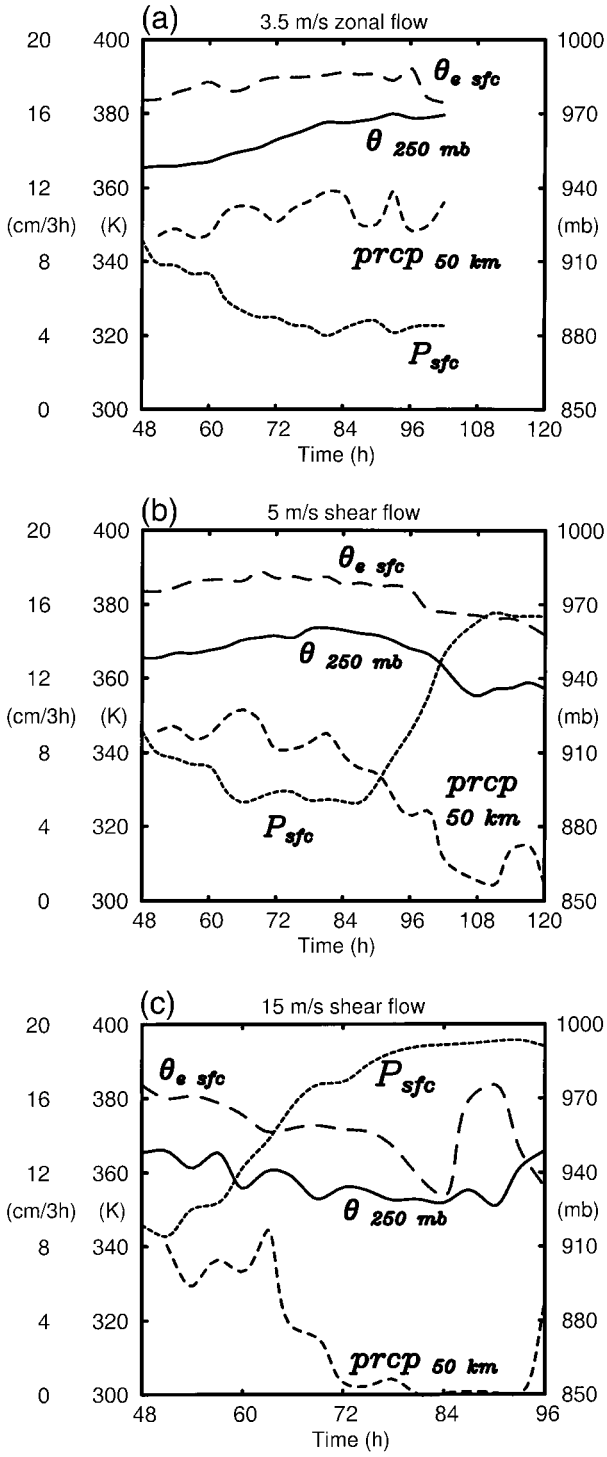

FIG. 15. Time series of maximum potential temperature at 250 mb (K, solid), maximum equivalent potential temperature at the surface (K, long dashes), minimum surface pressure (mb, short dashes), and previous 3-h rainfall averaged from 0- to 50-km radius [cm (3h)$^{-1}$, medium dashes], for the (a) 3.5, (b) 5 and (c) 15 m s^{-1} shear cases.

the surface also increase steadily, though by a slightly smaller amount than the upper-level temperature anomaly. The precipitation rate is more variable through the period than are the other quantities shown, but it too shows a slight increase with time.

The patterns are different in the two sheared cases. In the 5 m s^{-1} shear simulation the maximum θ at 250 mb appears to decrease by small amounts just before the central pressure begins to rise, although the surface value of θ_e remains nearly constant. Both quantities decrease more rapidly during the period of increasing cen-

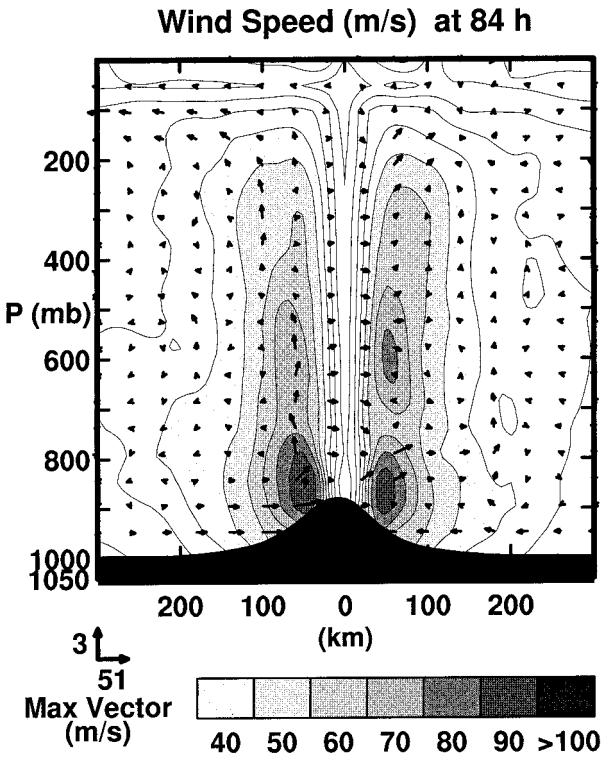

FIG. 16. Vertical cross sections of wind speeds plus vertical-radial wind vectors for the 3.5 m s^{-1} zonal flow case at $t = 84$ h.

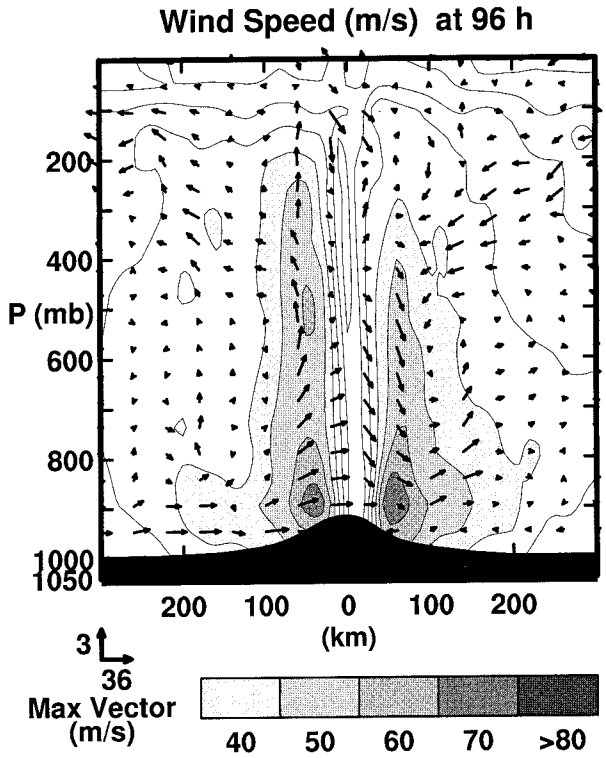

FIG. 17. As in Fig. 15 but for the 5 m s^{-1} shear case and at $t = 96$ h.

tral pressure, then level off as the pressure stabilizes around $t = 108$ h. In contrast, the rainfall rate remains steady for the first 24 h after the shear is added, but it then begins to decrease rapidly as the central pressure rises. There is relatively little rainfall still occurring in the inner 50 km by $t = 120$ h. This dramatic decrease in rainfall occurs as the eyewall becomes larger in diameter and its structure becomes highly asymmetric (see Fig. 8), with convection only occurring in small portions of the eyewall. The 15 m s^{-1} shear run shows similar relationships between the four quantities once the system begins to fill. The primary differences from the 5 m s^{-1} results are that the 15 m s^{-1} shear case begins filling much sooner (as noted above), and the rainfall in the core virtually disappears by $t = 72$ h. By that time this case has weakened to a loosely organized tropical storm with no trace of the eye–eyewall structure that is typical of a mature cyclone.

East–west vertical cross sections of the mean zonal flow case at $t = 84$ h, near the time of maximum intensity, are shown in Fig. 16. The tangential winds and radial-vertical velocity vectors show a strong, nearly vertical eyewall with classical tropical cyclone structure, including maximum winds near the top of the boundary layer and relatively weak vertical wind shear. Asymmetries in the wind field tend to be relatively small and reflect both standing and transient variations. The maximum θ anomaly is located near the 175-mb level (not shown) and is just over 20°C. The value of this maximum is realistic and consistent with the extremely low surface pressure, but the level at which it occurs seems relatively high compared to those seen in published eye analyses. However, there are few direct observations of eye properties at this level, and perhaps none in a storm this intense, so we will reserve judgement on whether the level of the anomaly is unrealistic. The cross section of θ suggests subsidence of stratospheric air into upper portions of the eye (see also Fig. 7). This process has been suggested by Holland (1997), and it could be that such subsidence is partially responsible for the high level at which the maximum θ anomaly occurs.

Similar cross sections are shown for the 5 m s^{-1} case at $t = 96$ h (Fig. 17) and for the 15 m s^{-1} shear case at $t = 60$ h (Fig. 18). These times correspond to periods of rapid filling for each case. The storm in 5 m s^{-1} shear (Fig. 17) maintains vertical alignment of the axis of rotation through a deep layer, but the eye shows strong asymmetries, particularly in the vertical motion and radial wind fields (see also Fig. 9d). The strongly sheared storm (Fig. 18) exhibits considerable tilt of the eyewall and strong asymmetries in both the tangential and vertical wind fields.

Finally, azimuthally averaged vertical cross sections of the horizontal eddy flux of equivalent potential temperature were computed by subtracting the product of the azimuthal means of the radial wind and θ_e from the

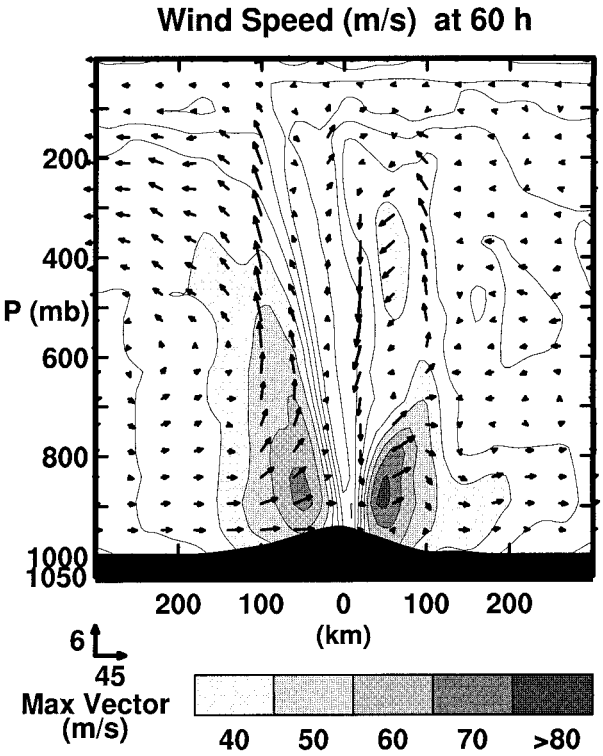

FIG. 18. As in Fig. 15 but for the 15 m s^{-1} shear case and at t = 60 h.

azimuthal means of the products of these variables at each height and radius. The resulting eddy fluxes are shown at 6-h intervals from t = 78 h through t = 108 h for the 5 m s^{-1} shear run (Fig. 19). Recall that this storm began to weaken at about t = 87 h (Fig. 4). The fluxes in Fig. 19 are very small at t = 78 h and at all previous times. However, just prior to the observed rise in central pressure (t = 84 h) the storm develops strong positive (outward) fluxes of θ_e in the eyewall region, including a local maximum centered around 250 mb. Although the pattern is not evident at t = 90 h, the subsequent time periods show outward eddy fluxes in the upper levels through t = 102 h. The patterns suggest that the level of maximum outward eddy flux descends with time, and the storm weakens throughout this period. At t = 108 h and thereafter, when the storm maintains a relatively steady intensity, there are no outward eddy fluxes in the upper levels. Thus, the eddy flux patterns are consistent with the view that upper-level asymmetries ventilate the eye, and that this process descends with time, during the period that the storm weakens.

4. Discussion

The results of the simulations of vortices in shear, when compared to the case of a vortex embedded in uniform zonal flow, indicate that the weakening of the storms in shear occurs according to the following scenario:

- The structure of the storm core, particularly the eyewall cloud region, develops strong wavenumber one asymmetries in vertical motion, cloud water, and rainwater at most levels almost immediately after the shear is applied. The convection and rainfall tend to become concentrated to the left of the shear vector. There are asymmetries in the tangential wind field as well, but they are much less pronounced and not as clearly related to the vertical shear. The relationships between wind distribution and vertical shear are being investigated and will be discussed in a future paper.
- The storm becomes sufficiently asymmetric so that in the upper layers the PV and θ_e anomalies lose their initial targetlike appearance, with maxima near the center of the eye, and develop a pattern with bands of maximum PV and θ_e concentrated only within the saturated portions of the eyewall and other rainbands. This change in structure occurs in conjunction with outward horizontal eddy fluxes of θ_e and PV. The maxima remain within the eye at middle and lower levels.
- The dissipation of the warm core structure at upper levels raises the surface pressure, weakening the circulation at all levels.
- The asymmetric pattern moves downward with time, so that the depth of the vortex that retains an erect vortex structure becomes shallower. The storm continues to weaken. Since the circulation is stronger at lower levels, the downward progression of the breakdown of the symmetric vortex may halt at some level, achieving an equilibrium structure at an intensity well below the storm's MPI.
- The sheared simulations develop a relatively steady intensity, but the 15 m s^{-1} shear case persists only as a weakly organized tropical storm–like system, while the 5 m s^{-1} case remains a minimal hurricane.

These results raise several questions. Two of these are, what causes the storm to lose its symmetric structure, and how does this weaken the storm? Montgomery and Kallenbach (1997) noted that wavenumber one asymmetries in dry, idealized hurricanes tend to weaken with time, as their energy is axisymmetrized into the mean vortex flow. The storms simulated here are able to maintain their strong, vertically aligned vortex structure despite asymmetries produced by the storm's motion. They are also able to maintain such a structure for some time when shear is applied—about a day and a half in 5 m s^{-1} shear, and about 24–30 h in 10 m s^{-1} shear. Hence, at least for the conditions simulated here, it would appear that the processes that tend to keep the storm axisymmetric are able to overcome shear at least temporarily for shears of less than 10 m s^{-1} or so. This result appears to agree with the observational studies discussed earlier.

As discussed earlier, there is uncertainty regarding

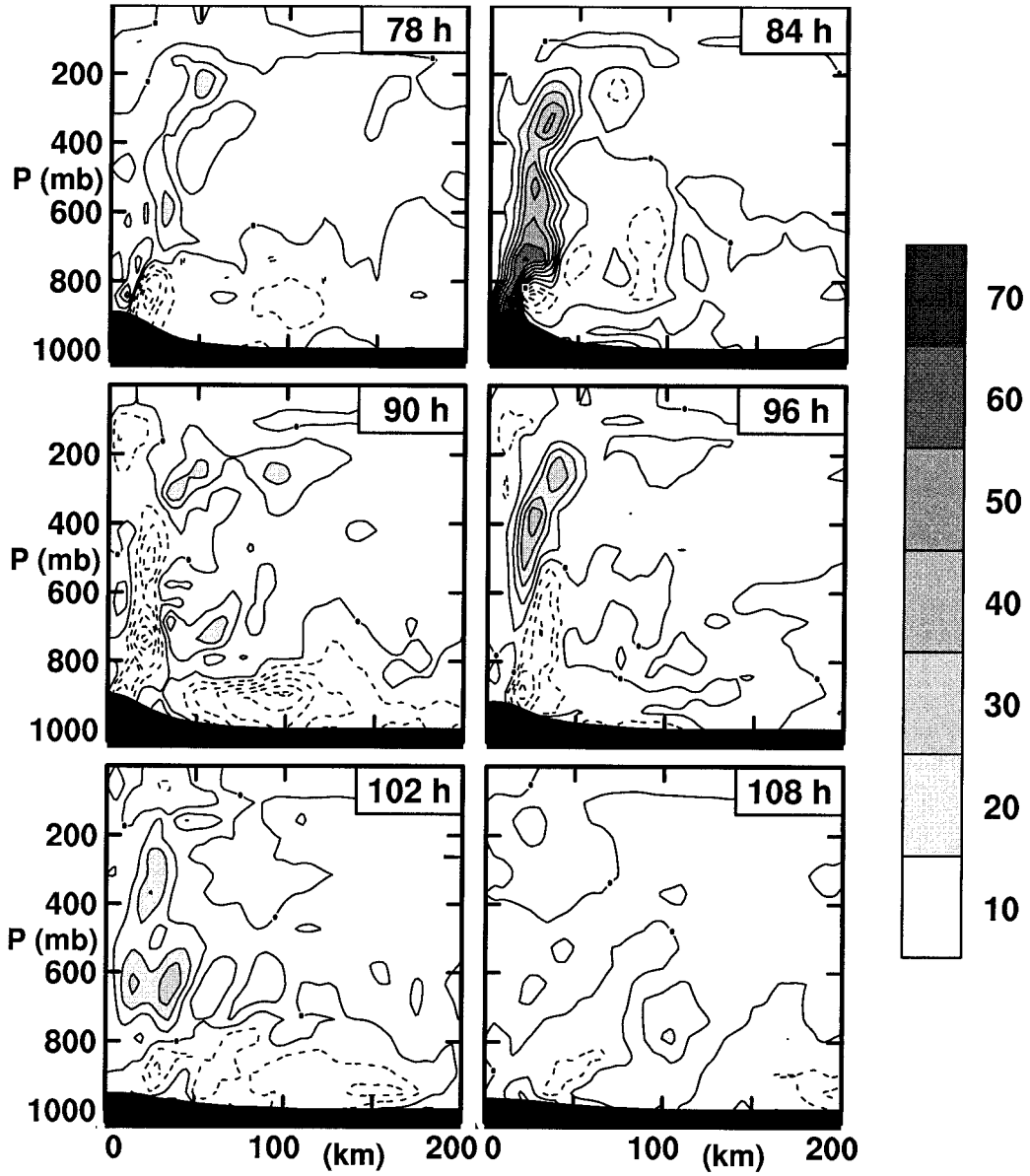

FIG. 19. Vertical-radius cross sections of the radial eddy fluxes of equivalent potential temperature (°C m s^{-1}) for the 5 m s^{-1} shear case at t = (a) 78, (b) 84, (c) 90, (d) 96, (e) 102, and (f) 108 h. The figure extends from the center of the storm to 200-km radius. Positive values (solid lines) denote outward fluxes. Dashed lines indicate negative values.

the relative importance of the various processes that act to transport PV into the eye from the eyewall, producing the vertically aligned, axisymmetric structure that is necessary to maintain an intense storm. The proposed mechanisms were filamentation, eyewall instability and breakdown, and turbulent mixing. We hypothesize that in a storm that has a symmetric eyewall structure, these processes combine to maintain the maxima of PV, θ_e, and related quantities with the eye, thus also maintaining the storm's intensity. When the storm becomes sufficiently asymmetric such that the processes that act to make the eyewall axisymmetric are unable to overcome the processes forcing the asymmetries in convection, the inward mixing processes cannot keep up with the ventilation of air in the eye caused by the shear. The warm core is rapidly advected away, as is the central PV anomaly. This happens first at upper levels, where the vortex is weakest and the inertial stability is smallest, but since the dissipation of the upper-level warm core also weakens the storm at lower levels, the process extends downward with time. This process is different from the mechanism proposed by DeMaria (1996), dis-

cussed earlier, in which core convection would be decreased due to vertical stability changes resulting by the shear-induced tilting of the vortex.

This argument also differs from that of Peng et al. (1999), who also found that wavenumber one asymmetries in eyewall structure tended to weaken their modeled storms once the asymmetries become sufficiently pronounced. They concluded that their storms weakened due to decoupling of the region of maximum surface fluxes from the region of maximum low-level convergence. Such decoupling was not observed in the current runs. However, not all aspects of the two studies are directly comparable, since Peng et al. (1999) did not impose vertical shear upon their storms other than that generated by the use of a variable Coriolis parameter.

It is clear that the subject of how the eyewall and the eye regions interact to maintain the types of structures observed in nature and in simulation results should be investigated further. However, due to the small scales of the processes involved, we propose to pursue such studies with a finer mesh version of the model than was available for the present study.

5. Conclusions

Simulations of tropical cyclones in idealized environments were performed using a nonhydrostatic model, a 5-km fine mesh, resolvable moist processes, and a constant Coriolis parameter. The model produced intense hurricane-like storms with intensities near their theoretical thermodynamic maximum values when placed in a zero-flow environment or within uniform easterly flow of 3.5 m s^{-1}. Although these storms developed wavenumber one asymmetries within their eyewall regions, the vortices were able to remain vertically aligned, with no resolvable tilt, and they maintained maxima of PV, θ, θ_e, etc. within their eyes. Hence, the tendency for the vortex to evolve toward axisymmetry was sufficient to overcome the small asymmetries produced by surface friction and the variability of convection.

When relatively weak (5 m s^{-1}) shear was added to the mean flow, the storms rapidly developed stronger wavenumber one asymmetries, with the maximum convection and rainfall concentrated to the left of the shear vector. The mechanism responsible for this asymmetry appears to be the differential vorticity advection with height caused by the shear, which in turn produces low-level convergence ahead of and to the left of the shear vector, with the air then rising in a cyclonic spiral, producing convection and rain on the left side of the shear vector. This view is in agreement with the arguments of Frank and Ritchie (1999) and is similar to the differential flow argument made earlier by Bender (1997). Since the vortex does not tilt appreciably until after the asymmetries develop, we feel that this mechanism predominates at least until such time as the storm does begin to lose its vertically erect structure.

While small-scale features of the asymmetries varied with time, the overall pattern was persistent, in agreement with other studies. However, the effects of the shear on storm intensity were not evident until about 36 h after the shear was imposed. This case eventually weakened and reached a relatively steady intensity of around 960 mb, still a hurricane but a far weaker one than it had been prior to the weakening. Moderate shear of 10 m s^{-1} affected the storm much as did the weaker 5 m s^{-1} shear except that the onset of the weakening began sooner (about 24 h after the shear was imposed), and the storm had not reached a steady intensity by the time it moved out of the fine mesh region. The delayed response of the storm's intensity to the shear suggests that the interaction between large-scale shear and storm intensity may be more complex than previously thought, at least for weak to moderate shears. This topic should be investigated further using both models and observations. Such lags in response to shear changes may be obscuring analyses of the effects of shear on storm intensity.

Strong shear of 15 m s^{-1} literally tore an intense storm apart within about one day. Observational studies have suggested that shears on the order of 10 m s^{-1} are strong enough to have major adverse effects on storm intensity (e.g., Zehr, 1992), and the results of the present study suggest a threshold value somewhere between about 10 and 15 m s^{-1}, at least for rapid response of intensity to shear.

The simulated storms weaken from the top downward, with the shear dissipating the warm air and potential vorticity anomalies in the upper layers, leading to overall weakening of the storm, followed by a breakdown of the symmetric vortex at lower levels. If this is found to be true of storms in nature as well, it suggests that one might be able to monitor and forecast storm intensity from observations of the core properties at upper levels. Such observations are not easy to obtain at present, but future sensors might be developed with those capabilities. The modeled storms appear to ventilate the upper portions of the eye due to asymmetric circulations, thereby weakening the storm pressure anomaly. This process appears to differ from the mechanism proposed by DeMaria (1996), which involved balanced vortex response to tilt of the vortex by shear and an accompanying drop in midlevel temperatures in the eye. The relationships between the two arguments will be studied in future work.

Since all of the simulations in this study are performed with a fixed sea surface temperature, the changes that occur during the sheared simulations can be attributed primarily to the effects of the shear. The results suggest that wind shears in the 5–15 m s^{-1} range can cause major changes in hurricane intensity and structure, which is in agreement with available observations. This does not imply that shear effects dominate over ocean interaction effects in governing hurricane intensity in nature, but since shears of this magnitude are relatively

common, the results suggest that shear plays a major role in determining the evolution of many real hurricanes.

Much work remains to be done, including expanding the work to include variable f, finer grid resolutions (1–2 km) capable of better resolving eyewall eddies, and more complex environments. A study examining effects of multidirectional shear is now in progress, and the effects of the shape of the vertical shear profile on the results also needs to be studied further. The work should be expanded to include real-data cases that can be initialized and verified with special datasets. We are currently engaged in such research and will report on the results in the near future. However, even at this stage of the research, the results of this and other referenced studies suggest that the relationships between large-scale vertical shear and the intensity and structure of tropical cyclones are strong and persistent. Since the large-scale flow itself is assumed to be predictable, we conclude that the structures and intensities of tropical cyclones are also predictable. Hence, the way seems open to develop a new generation of high-resolution tropical cyclone models that would produce useful forecasts of storm winds, pressures, and rainfall. We encourage the application of this work to the development of improved forecast guidance products, and we plan to pursue research in that area as well.

Acknowledgments. This work was supported by grants from the National Science Foundation (Grants ATM-9908020 and ATM-9714253) and the Office of Naval Research (Grant N0001499WR30003). The authors are grateful to Professors Craig Bishop and Jenni Evans for their helpful discussions during the research. They also wish to thank Drs. Chris Landsea and Mark DeMaria and an anonymous reviewer for their constructive comments on the earlier version of the manuscript.

REFERENCES

Bender, M. A., 1997: The effect of relative flow on the asymmetric structure of the interior of hurricanes. *J. Atmos. Sci.,* **54,** 703–724.

Betts, A. K., and M. Miller, 1986: A new convective adjustment scheme, Part II: Single column tests using GATE wave, BOMEX, ATEX and arctic air-mass data sets. *Quart. J. Roy. Meteor. Soc.,* **112,** 693–709.

Black, P. G., and F. D. Marks, 1991: The structure of an eyewall meso-vortex in Hurricane Hugo (1989). Preprints, *19th Conf. on Hurricanes and Tropical Meteorology*, Miami, FL, Amer. Meteor. Soc., 579–582.

DeMaria, M., 1996: The effect of vertical shear on tropical cyclone intensity change. *J. Atmos. Sci.,* **53,** 2076–2087.

——, and J. Kaplan, 1994: Sea surface temperature and the maximum intensity of Atlantic tropical cyclones. *J. Climate,* **7,** 1324–1334.

——, and ——, 1999: An updated Statistical Hurricane Intensity Prediction Scheme (SHIPS) for the Atlantic and eastern North Pacific basins. *Wea. Forecasting,* **14,** 326–337.

Drury, S., and J. L. Evans, 1998: Modeling of tropical cyclone intensification as a result of interaction with mid-latitude troughs. Preprints, *Symp. on Tropical Cyclone Intensity Change,* Phoenix, AZ, Amer. Meteor. Soc., 65–72.

Dudhia, J., 1989: Numerical study of convection observed during the Winter Monsoon Experiment using a mesoscale two-dimensional model. *J. Atmos. Sci.,* **46,** 3077–3107.

Emanuel, K. A., 1988: The maximum intensity of hurricanes. *J. Atmos. Sci.,* **45,** 1143–1155.

——, 1999: Thermodynamic control of hurricane intensity. *Nature,* **401,** 665–669.

Frank, W. M., 1998: Mechanisms of environmentally induced hurricane structure change. Preprints, *Symp. on Tropical Cyclone Intensity Change,* Phoenix, AZ, Amer. Meteor. Soc., 15–20.

——, and E. A. Ritchie, 1997: Environmental effects on the structure of tropical storms. Preprints, *22d Conf. on Hurricanes and Tropical Meteorology,* Fort Collins, CO, Amer. Meteor. Soc., 352–353.

——, and ——, 1999: Effects on environmental flow upon tropical cyclone structure. *Mon. Wea. Rev.*, **127,** 2044–2061.

Franklin, J. L., S. J. Lord, S. E. Feuer, and F. D. Marks Jr., 1993: The kinematic structure of Hurricane Gloria (1985) determined form nested analyses of dropwinsonde and Doppler wind data. *Mon. Wea. Rev.*, **121,** 2433–2451.

Gray, W. M., 1968: Global view of the origin of tropical disturbances and storms. *Mon. Wea. Rev.*, **96,** 669–700.

——, 1979: Hurricanes, their formation, structure, and likely role in the tropical circulation. *Meteorology over the Tropical Oceans,* D. B. Shaw, Ed., Royal Meteorological Society, 155–218.

Holland, G. J., 1997: The maximum potential intensity of tropical cyclones. *J. Atmos. Sci.,* **54,** 2519–2541.

Jones, S. C., 1995: The evolution of vortices in vertical shear. Part I: Initially barotropic vortices. *Quart. J. Roy. Meteor. Soc.,* **121,** 821–851.

Marks, F. D., Jr., R. A. Houze Jr., and J. F. Gamache, 1992: Dual-aircraft investigation of the inner core of Hurricane Norbert. Part I: Kinematic structure. *J. Atmos. Sci.,* **49,** 919–942.

McBride, J. L., and R. M. Zehr, 1981: Observational analysis of tropical cyclone formation. Part II: Comparison of non-developing versus developing systems. *J. Atmos. Sci.,* **38,** 1132–1151.

Moeller, D. J., and M. T. Montgomery, 1999: Vortex Rossby waves and hurricane intensification in a barotropic model. *J. Atmos. Sci.,* **56,** 1674–1687.

Montgomery, M. T., and R. J. Kallenbach, 1997: A theory for vortex Rossby waves and its application to spiral bands and intensity changes in hurricanes. *Quart. J. Roy. Meteor. Soc.,* **123,** 535–565.

Peng, M. S., B.-F. Jeng, and R. T. Williams, 1999: A numerical study on tropical cyclone intensification. Part I: Beta effect and mean flow effect. *J. Atmos. Sci.,* **56,** 1404–1423.

Ritchie, E. A., and G. J. Holland, 1997: Scale interactions during the formation of Typhoon Irving. *Mon. Wea. Rev.,* **125,** 1377–1396.

Schubert, W. H., M. T. Montgomery, R. K. Taft, T. A. Guinn, S. R. Fulton, J. P. Kossin, and J. P. Edwards, 1999: Polygonal eyewalls, asymmetric eye contraction, and potential vorticity mixing in hurricanes. *J. Atmos. Sci.,* **56,** 1197–1223.

Shafran, P. C., N. L. Seaman, and G. A. Gayno, 2000: Evaluation of numerical prediction of boundary layer structure during the Lake Michigan Ozone Study (LMOS). *J. Appl. Meteor.*, **39,** 412–426.

Shapiro, L. J., 1983: The asymmetric boundary layer flow under a translating hurricane. *J. Atmos. Sci.,* **40,** 1984–1998.

Tuleya, R. E., and Y. Kurihara, 1981: A numerical study on the effects of environmental flow on tropical cyclone genesis. *Mon. Wea. Rev.,* **109,** 2487–2506.

Willoughby, H. E., 1995: Mature structure and evolution. *Global Perspectives on Tropical Cyclones,* R. L. Elsberry, Ed., World Meteorological Organization Rep. TCP-38, 21–62.

Zehr, R. M., 1992: Tropical cyclogenesis in the western North Pacific. NOAA Tech. Rep. NESDIS 61, 181 pp. [Available from NOAA/NESDIS, E/RA22, 5200 Auth Road, Washington, DC 20233.]